genetic variants we also investigated their liver and kidney uptake clearances (Table 1). No clear correlation could be found between organ uptakes and changes in protein charge or hydrophobicity, respectively. With respect to the effect of changes in α-helical content the domains again behaved differently. For changes in domains I and III good correlations were found ($P=0.1-0.2$) between increases in percent change of α-helical content and decreases in the change of liver (Fig. 3B) and kidney (Fig. 3C) uptakes. For domain II changes, a good correlation ($P=0.1$) was observed for kidney uptake (Fig. 3F), whereas no correlation was registered between the molecular alterations and changes in liver uptake clearance (Fig. 3E). As with the plasma half-lives, no correlations were found between changes in organ uptakes and changes in ΔH_v (Fig. 4B, C, E and F).

Uptake of HSA by liver and kidneys is mainly due to the presence of cell membrane receptors which recognize the protein and then internalize it by endocytosis. Hepatocytes and the nonparenchymal cells of the liver are involved in galactosyl receptor-mediated and mannose receptor-mediated endocytosis, respectively. Due to the specificities of these receptors, it is not likely that the effects of the present single-residue mutations on liver uptake clearance can be explained by one of these mechanisms. The liver also possesses receptors for rapid uptake of oxidized albumin and albumin with advanced glycation end products. Whether small molecular changes such as single-residue mutations can initiate endocytosis by scavenger receptors such as gp18 or gp30 is at present only speculative. On the other hand, liver uptake by adsorptive endocytosis could be influenced by the amino acid substitutions, because this type of uptake is dependent on the net charge of the protein.

Normally, glomerular filtration of HSA in the kidneys is followed by its return into the venous circulation without degradation (the albumin retrieval pathway). However, a small fraction is degraded in proximal tubular cells most probably after uptake by the endocytic receptors megalin and cubulin. Whether genetic modification of HSA results in increased glomerular filtration and increased uptake by this receptor-complex remains to be clarified. It should be noted that no radioactivity was detected in the urine during the present experimental time. An alternative explanation for the increased uptake of the albumin isoforms by the kidney could be uptake by tubular receptors for advanced glycation end products (RAGE-receptors). As with the scavenger receptors of the liver, it is not known whether single-residue mutations of HSA can initiate uptake by these receptors.

Fujino et al. [37] have found that oxidized bovine serum albumin, in contrast to the native protein, can be cleaved by oxidized protein hydrolase. Because this endopeptidase is found in the blood, it could partly hydrolyse some of the genetic variants in the mouse circulation and thereby render them more exposed to organ uptake. The enzyme selectively recognizes hydrophobic regions in its substrate. Therefore, this mechanism can be especially relevant for the genetic variants with increased hydrophobicity, which all have shorter plasma half-lives (Tables 1 and 2).

More recently, another type of endocytosis of HSA has been identified in virtually all nucleated cells which results in reuse of the protein [38]. After pinocytosis, albumin binds intracellularly and in a pH-dependent manner to the receptor FcRn. Thereby the protein is diverted from the lysosomal degradation pathway and exocytosed back to the circulation in an intact form extending its plasma half-life. Chaudhury et al. [39] have proposed that the intracellular binding of HSA to FcRn is caused by interaction(s) between histidine residue(s) in the receptor and histidine residues in domain III of albumin. By contrast, Andersen et al. [40] suggested that FcRn interacts with negatively charged and surface exposed residues on domain III of HSA. Thus, especially genetic variants with domain III substitutions could have modified plasma half-lives due to a modified HSA-FcRn recycling process.

In conclusion, the plasma half-life of HSA can be modified by single-residue mutations on its surface. No clear relation exists with respect to type of mutation, but +2 variants increase the half-life, whereas increased hydrophobicity decreases it. Changes in the proteins α-helical content have a positive effect on the half-life, if they take place in domain I or III, else they have a negative effect (domain II). By contrast, no correlation was found between the half-lives and changes in ΔH_v representing thermal stability. All mutations modified liver and kidney uptake clearances, and good correlations were found when relating liver (partly) and kidney uptakes to changes in α-helical content. No correlations were found to type of mutation, changes in charge or hydrophobicity or to changes in ΔH_v. Organ uptakes are brought about by different types of endocytosis with different characteristics. Some of these lead to protein destruction in the lysosomes, whereas interaction with FcRn results in recycling of HSA. The relatively few correlations between molecular albumin parameters and organ uptakes could be due to different effects of the mutations on the various forms of endocytosis. However, substitutions of domain III of HSA could modify binding to FcRn and thereby alter its recycling. Although several details with respect to organ uptakes still have to be shed light on, the present information should be useful when designing recombinant HSA mutants with a modified plasma half-life.

Acknowledgements

This work was supported, in part, by Grants-in-Aid for Scientific Research from the Ministry of Education, Science, Sports and Culture of Japan (14370759) and by Fonden af 1870.

References

[1] U. Kragh-Hansen, Molecular aspects of ligand binding to serum albumin, Pharmacol. Rev. 33 (1981) 17–53.
[2] T. Peters Jr., All About Albumin: Biochemistry, Genetics, and Medical Applications, Academic Press, San Diego, CA, 1996.
[3] D.C. Carter, J.X. Ho, Structure of serum albumin, Adv. Protein Chem. 45 (1994) 153–203.
[4] S. Sugio, A. Kashima, S. Mochizuki, M. Noda, K. Kobayashi, Crystal structure of human serum albumin at 2.5 A resolution, Protein Eng. 12 (1999) 439–446.
[5] P. Yeh, D. Landais, M. Lemaitre, I. Maury, J.Y. Crenne, J. Becquart, A. Murry-Brelier, F. Boucher, G. Montay, R. Fleer, P.-H. Hirel, J.-F. Mayaux, D. Klatzmann, Design of yeast-secreted albumin derivatives for human therapy: biological and antiviral properties of a serum albumin-CD4 genetic conjugate, Proc. Natl. Acad. Sci. U. S. A. 89 (1992) 1904–1908.

[6] S. Syed, P.D. Schuyler, M. Kulczycky, W.P. Sheffield, Potent antithrombin activity and delayed clearance from the circulation characterize recombinant hirudin genetically fused to albumin, Blood 89 (1997) 3243–3252.
[7] Y. Yamasaki, K. Sumimoto, M. Nishikawa, F. Yamashita, K. Yamaoka, M. Hashida, Y. Takakura, Pharmacokinetic analysis of in vivo disposition of succinylated proteins targeted to liver nonparenchymal cells via scavenger receptors: importance of molecular size and negative charge density for in vivo recognition by receptors, J. Pharmacol. Exp. Ther. 301 (2002) 467–477.
[8] S.F. Ma, M. Nishikawa, H. Katsumi, F. Yamashita, M. Hashida, Cationic charge-dependent hepatic delivery of amidated serum albumin, J. Control Release 102 (2005) 583–594.
[9] Y. Iwao, M. Anraku, K. Yamasaki, U. Kragh-Hansen, K. Kawai, T. Maruyama, M. Otagiri, Oxidation of Arg-410 promotes the elimination of human serum albumin, Biochim. Biophys. Acta 1764 (2006) 743–749.
[10] L. Minchiotti, M. Campagnoli, A. Rossi, M.E. Cosulich, M. Monti, P. Pucci, U. Kragh-Hansen, B. Granel, P. Disdier, P.J. Weiller, M. Galliano, A nucleotide insertion and frameshift cause albumin Kenitra, an extended and O-glycosylated mutant of human serum albumin with two additional disulfide bridges, Eur. J. Biochem. 268 (2001) 344–352.
[11] U. Kragh-Hansen, S. Saito, K. Nishi, M. Anraku, M. Otagiri, Effect of genetic variation on the thermal stability of human serum albumin, Biochim. Biophys. Acta 1747 (2005) 81–88.
[12] M. Galliano, L. Minchiotti, P. Iadarola, G. Ferri, M.C. Zapponi, A.A. Castellani, The amino acid substitution in albumin Roma: 321 Glu → Lys, FEBS Lett. 233 (1988) 100–104.
[13] L. Minchiotti, M. Galliano, M. Stoppini, G. Ferri, H. Crespeau, D. Rochu, F. Porta, Two alloalbumins with identical electrophoretic mobility are produced by differently charged amino acid substitutions, Biochim. Biophys. Acta 1119 (1992) 232–238.
[14] D. Savva, A.L. Tarnoky, M.F. Vickers, Genetic characterization of an alloalbumin, albumin Kashmir, using gene amplification and allele-specific oligonucleotides, Biochem. J. 266 (1990) 615–617.
[15] L. Minchiotti, M. Galliano, P. Iadarola, M. Stoppini, G. Ferri, A.A. Castellani, Structural characterization of two genetic variants of human serum albumin, Biochim. Biophys. Acta 916 (1987) 411–418.
[16] Y. Sakamoto, K. Kitamura, J. Madison, S. Watkins, C.B. Laurell, M. Nomura, T. Higashiyama, F.W. Putnam, Structural study of the glycosylated and unglycosylated forms of a genetic variant of human serum albumin (63 Asp → Asn), Biochim. Biophys. Acta 1252 (1995) 209–216.
[17] O. Sugita, N. Endo, T. Yamada, M. Yakata, S. Odani, The molecular abnormality of albumin Niigata: 269 Asp → Gly, Clin. Chim. Acta 164 (1987) 251–259.
[18] L. Minchiotti, U. Kragh-Hansen, H. Nielsen, E. Hardy, A.Y. Mercier, M. Galliano, Structural characterization, stability and fatty acid-binding properties of two French genetic variants of human serum albumin, Biochim. Biophys. Acta 1431 (1999) 223–231.
[19] S.O. Brennan, The molecular abnormality of albumin Parklands: 365 Asp → His, Biochim. Biophys. Acta 830 (1985) 320–324.
[20] M. Galliano, S. Watkins, J. Madison, F.W. Putnam, U. Kragh-Hansen, R. Cesati, L. Minchiotti, Structural characterization of three genetic variants of human serum albumin modified in subdomains IIB and IIIA, Eur. J. Biochem. 251 (1998) 329–334.
[21] L. Minchiotti, S. Watkins, J. Madison, F.W. Putnam, U. Kragh-Hansen, A. Amoresano, P. Pucci, R. Cesati, M. Galliano, Structural characterization of four genetic variants of human serum albumin associated with alloalbuminemia in Italy, Eur. J. Biochem. 247 (1997) 476–482.
[22] J. Madison, M. Galliano, S. Watkins, L. Minchiotti, F. Porta, A. Rossi, F.W. Putnam, Genetic variants of human serum albumin in Italy: point mutants and a carboxyl-terminal variant, Proc. Natl. Acad. Sci. U. S. A. 91 (1994) 6476–6480.
[23] S.O. Brennan, P. Herbert, Albumin Canterbury (313 Lys → Asn). A point mutation in the second domain of serum albumin, Biochim. Biophys. Acta 912 (1987) 191–197.
[24] L. Minchiotti, M. Galliano, M.C. Zapponi, R. Tenni, The structural characterization and bilirubin-binding properties of albumin Herborn, a [Lys240 → Glu] albumin mutant, Eur. J. Biochem. 214 (1993) 437–444.
[25] K. Arai, K. Huss, J. Madison, F.W. Putnam, F.M. Salzano, M.H. Franco, S.E. Santos, M.J. Freitas, Amino acid substitutions in albumin variants found in Brazil, Proc. Natl. Acad. Sci. U. S. A. 86 (1989) 1821–1825.
[26] E.K. Chua, S.O. Brennan, P.M. George, Albumin Church Bay: 560 Lys → Glu a new mutation detected by electrospray ionisation mass spectrometry, Biochim. Biophys. Acta 1382 (1998) 305–310.
[27] P. Iadarola, L. Minchiotti, M. Galliano, Localization of the amino acid substitution site in a fast migrating variant of human serum albumin, FEBS Lett. 180 (1985) 85–88.
[28] S.O. Brennan, A.P. Fellowes, Albumin Hawkes Bay; a low level variant caused by loss of a sulphydryl group at position 177, Biochim. Biophys. Acta 1182 (1993) 46–50.
[29] U. Kragh-Hansen, A micromethod for delipidation of aqueous proteins, Anal. Biochem. 210 (1993) 318–327.
[30] R.F. Chen, Removal of fatty acids from serum albumin by charcoal treatment, J. Biol. Chem. 242 (1967) 173–181.
[31] D.J. Hnatowich, W.W. Layne, R.L. Childs, The preparation and labeling of DTPA-coupled albumin, Int. J. Appl. Radiat. Isot. 33 (1982) 327–332.
[32] F. Staud, M. Nishikawa, K. Morimoto, Y. Takakura, M. Hashida, Disposition of radioactivity after injection of liver-targeted proteins labeled with ^{111}In or ^{125}I. Effect of labeling on distribution and excretion of radioactivity in rats, J. Pharm. Sci. 88 (1999) 577–585.
[33] J.R. Duncan, M.J. Welch, Intracellular metabolism of indium-111-DTPA-labeled receptor targeted proteins, J. Nucl. Med. 34 (1993) 1728–1738.
[34] K. Yamaoka, Y. Tanigawara, T. Nakagawa, T. Uno, A pharmacokinetic analysis program (multi) for microcomputer, J. Pharmacobio-Dyn. 4 (1981) 879–885.
[35] W.P. Sheffield, J.A. Marques, V. Bhakta, I.J. Smith, Modulation of clearance of recombinant serum albumin by either glycosylation or truncation, Thromb. Res. 99 (2000) 613–621.
[36] K. Nakajou, H. Watanabe, U. Kragh-Hansen, T. Maruyama, M. Otagiri, The effect of glycation on the structure, function and biological fate of human serum albumin as revealed by recombinant mutants, Biochim. Biophys. Acta 1623 (2003) 88–97.
[37] T. Fujino, M. Kojima, M. Beppu, K. Kikugawa, H. Yasuda, K. Takahashi, Identification of the cleavage sites of oxidized protein that are susceptible to oxidized protein hydrolase (OPH) in the primary and tertiary structures of the protein, J. Biochem. (Tokyo) 127 (2000) 1087–1093.
[38] C. Chaudhury, S. Mehnaz, J.M. Robinson, W.L. Hayton, D.K. Pearl, D.C. Roopenian, C.L. Anderson, The major histocompatibility complex-related Fc receptor for IgG (FcRn) binds albumin and prolongs its lifespan, J. Exp. Med. 197 (2003) 315–322.
[39] C. Chaudhury, C.L. Brooks, D.C. Carter, J.M. Robinson, C.L. Anderson, Albumin binding to FcRn: distinct from the FcRn–IgG interaction, Biochemistry 45 (2006) 4983–4990.
[40] J.T. Andersen, J. Dee Qian, I. Sandlie, The conserved histidine 166 residue of the human neonatal Fc receptor heavy chain is critical for the pH-dependent binding to albumin, Eur. J. Immunol. 36 (2006) 3044–3051.

Original Article

Effect of Olmesartan on Oxidative Stress in Hemodialysis Patients

Daisuke KADOWAKI[1], Makoto ANRAKU[1], Yuka TASAKI[1], Kenichiro KITAMURA[2], Shiho WAKAMATSU[2], Kimio TOMITA[2], Janusz M. GEBICKI[3], Toru MARUYAMA[1], and Masaki OTAGIRI[1]

The effect of olmesartan, an inverse angiotensin II type 1 receptor blocker (ARB), on oxidative stress in hemodialysis (HD) patients is not fully understood, and has not been widely investigated *in vitro* or *in vivo*. We determined the amount of oxidized albumin and albumin hydroperoxides formed during incubation in the absence and presence of olmesartan by high-performance liquid chromatography (HPLC) and by a ferrous oxidation xylenol assay in an *in vitro* study. Six hypertensive HD patients were treated with 40 mg of olmesartan once daily, and blood pressure monitoring (BPM) was performed after 0, 4, and 8 weeks of treatment. The ratio of oxidized to unoxidized albumin was also determined. The oxidized albumin ratios and levels of albumin hydroperoxides were significantly decreased in a concentration-dependent manner in the presence of olmesartan, compared with the absence of olmesartan ($p<0.05$) in *in vitro* studies. In HD patients, olmesartan also significantly reduced systolic and diastolic blood pressure after 4 weeks, with a further significant decrease after 8 weeks. The ratio of oxidized to unoxidized albumin was markedly decreased after 4 weeks and these lower levels were maintained at 8 weeks. Olmesartan effectively lowered the extent of oxidation of albumin in both *in vitro* and *in vivo* studies, and this effect might confer benefits beyond a reduction in blood pressure. (*Hypertens Res* 2007; 30: 395–402)

***Key Words*: olmesartan, blood pressure, oxidative stress, hemodialysis, albumin**

Introduction

The renin-angiotensin-aldosterone system (RAAS) plays an important role in regulating blood pressure (BP). Angiotensin II type 1 (AT1) receptor blockers (ARBs) inhibit the RAAS and have been shown to be effective for treating hypertension (*1*, *2*). Independent of their ability to lower BP, these compounds have also been reported to reduce the progression of nephropathy in patients with diabetes mellitus (DM) and chronic kidney disease (CKD) (*3–5*). Although much of the renal protective effects of ARBs might be due to the lowering of BP, some protection may be due to their effects in reducing oxidative stress. In support of this idea, the blocking of AT1 receptors in hypertensive patients has been shown to reduce oxidative stress, inflammation, and endothelial dysfunction (*6*).

The mechanisms associated with hypertension in hemodialysis (HD) patients are complex, but the RAAS is generally thought to be an important contributor. Angiotensin II, *via* AT1 receptor, stimulates nicotinamide adenine dinucleotide phosphate (NADPH) oxidase and enhances the production of reactive oxygen species (*7*), which in turn contributes to endothelial dysfunction and vascular inflammation (*8*, *9*). Thus, the combination of hypertension and oxidative stress induced by stimulation of the RAAS results in the accelerated progression of atherosclerosis in HD patients (*10*).

Olmesartan is an orally active nonpeptide ARB that lowers

From the [1]Department of Biopharmaceutics, Graduate School of Pharmaceutical Sciences and [2]Department of Nephrology, Graduate School of Medical Sciences, Kumamoto University, Kumamoto, Japan; and [3]Department of Biological Sciences, Macquarie University, Sydney, Australia.

Address for Reprints: Masaki Otagiri, Ph.D., Department of Biopharmaceutics, Graduate School of Pharmaceutical Sciences, Kumamoto University, 5–1 Oe-honmachi, Kumamoto 862–0973, Japan. E-mail: otagirim@gpo.kumamoto-u.ac.jp

Received October 10, 2006; Accepted in revised form December 26, 2006.

BP when administered daily. Due to its long duration of action, BP control is maintained throughout 24 h. The antihypertensive efficacy and excellent tolerability of olmesartan have been demonstrated in short-term and long-term controlled trials (*11–14*). Miyata *et al.* recently reported that olmesartan, unlike a calcium channel blocker (CCB), inhibited the formation of advanced glycation end-products (AGE) in an *in vitro* study. Olmesartan is a biphenyl tetrazole derivative with a common core structure, 5-(4′-methylbiphenyl-2-yl)-1H-tetrazol, and this core structure is probably responsible for the inhibitory effect on oxidative stress (*15*). Thus, this effect suggests that olmesartan exhibits antioxidant activity in addition to reducing BP. However, the antioxidant effects of olmesartan have not been extensively studied either *in vitro* or *in vivo*.

The aim of this study was to examine the possible antioxidant and free radical-scavenging properties of olmesartan in *in vitro* studies. We also evaluated the effect of once daily administration of 40 mg of olmesartan on BP and on oxidized serum albumin, a marker of protein oxidation, in HD patients (*16–18*).

Methods

Patients

The study protocol was approved by the Institutional Review Board of Kumamoto University. Patients who met each of the following criteria were included in the study: 1) predialysis BP > 140/90 mmHg for 6 consecutive dialysis sessions; 2) no prior treatment with RAAS inhibitors; 3) stable weight for at least 3 months before enrollment; 4) weight gain of less than 5% between dialysis sessions. Written informed consent was obtained from each of 6 stable HD patients (4 men, 2 women) aged 37–80 (mean, 55.5±6.4) years with a duration of dialysis under 1 year. The cause of end-stage renal disease was glomerulonephritis in all cases. At enrollment, all patients were on regular bicarbonate HD for 4–5 h 3 times weekly using high-flux polysulfone hollow-fiber dialyzers. They were not treated with antioxidants such as vitamin E and C or with intravenous iron supplements during the 3 months before inclusion in the study.

Study Design

The study consisted of a 4-week placebo baseline period followed by an 8-week, open-label active treatment period during which the patients received olmesartan once daily, in the morning, at a dose of 40 mg. In patients already on CCB therapy, olmesartan was added to the previous drug. After 0, 4, and 8 weeks of olmesartan therapy, blood samples were obtained from each patient before the first HD session of the week for measurement of the ratio of oxidized to unoxidized albumin. In addition, blood pressure monitoring (BPM) was performed for each patient after 0, 4, and 8 weeks. To avoid any bias with respect to body fluid condition and dialysis efficiency, BPM was performed on the first non-dialysis day after the first HD session of the week. The drugs, dialysis conditions and dry weight of each patient were not changed during either the 4-week placebo period or 8-week treatment period.

Materials and Reagents

Human serum albumin (HSA; Cohn fraction V, fat free) and catalase (EC 1.11.1.6; 65,000 U/mg) were supplied by Boehringer-Mannheim (Mannheim, Germany). Xylenol orange (*o*-cresosulfonaphthalein-3,3-bis-[sodium methyliminodiacetate]) was from Sigma (St. Louis, USA). Olmesartan was obtained from Sankyo Pharmaceutical (Tokyo, Japan).

Chromatography of Serum Albumin

High-performance liquid chromatography (HPLC) was used to analyze serum albumin as described previously (*16*). Samples obtained from the *in vitro* study and from each patient were immediately frozen and stored at −80°C until used for analysis. Then 5 μL aliquots of serum were analyzed on a Shodex Asahipak ES-502N column (Showa Denko Co., Ltd., Tokyo, Japan). From the HPLC profile, the content of each albumin fraction (human mercaptalbumin, f[HMA]; human nonmercaptalbumin-1, f[HNA-1]; human nonmercaptalbumin-2, f[HNA-2]) was estimated as the area of the HNA fraction divided by the HMA fraction of the serum albumin peak (*17*).

Antioxidant Activity of Olmesartan *In Vitro*

Incubation Assay

Fresh heparinized plasma samples were obtained from uremic patients, with informed consent, before the dialysis session. To achieve adequate volumes of plasma and to obtain a stable baseline in experiments in which multiple results were generated, *in vitro* experiments were performed with plasma pooled from several donors ($n=3$ to $n=5$). Pooled plasma (900 μL) was incubated with olmesartan in the presence of air at 37°C. The drug was dissolved in ethanol to obtain a stock solution of 200 μmol/L and further diluted to the required concentrations. One milliliter samples of the plasma were incubated in the presence of air at 37°C for 7 days in the presence of the tested compounds (final concentrations: 2.0 and 20 μmol/L). At the end of the incubation, the ratio of oxidized to control albumin was measured, as described before.

Protein Hydroperoxides

Protein hydroperoxides were generated by irradiating 20 μmol/L HSA solutions with ^{60}Co γ-rays at a dose rate of 36 Gy/min. Protein hydroperoxides were measured by the perchloric acid–xylenol orange assay (*19*). The radiation-generated H_2O_2 was removed by treatment with catalase (154 U/mL). After the addition of the assay reagents and standing at

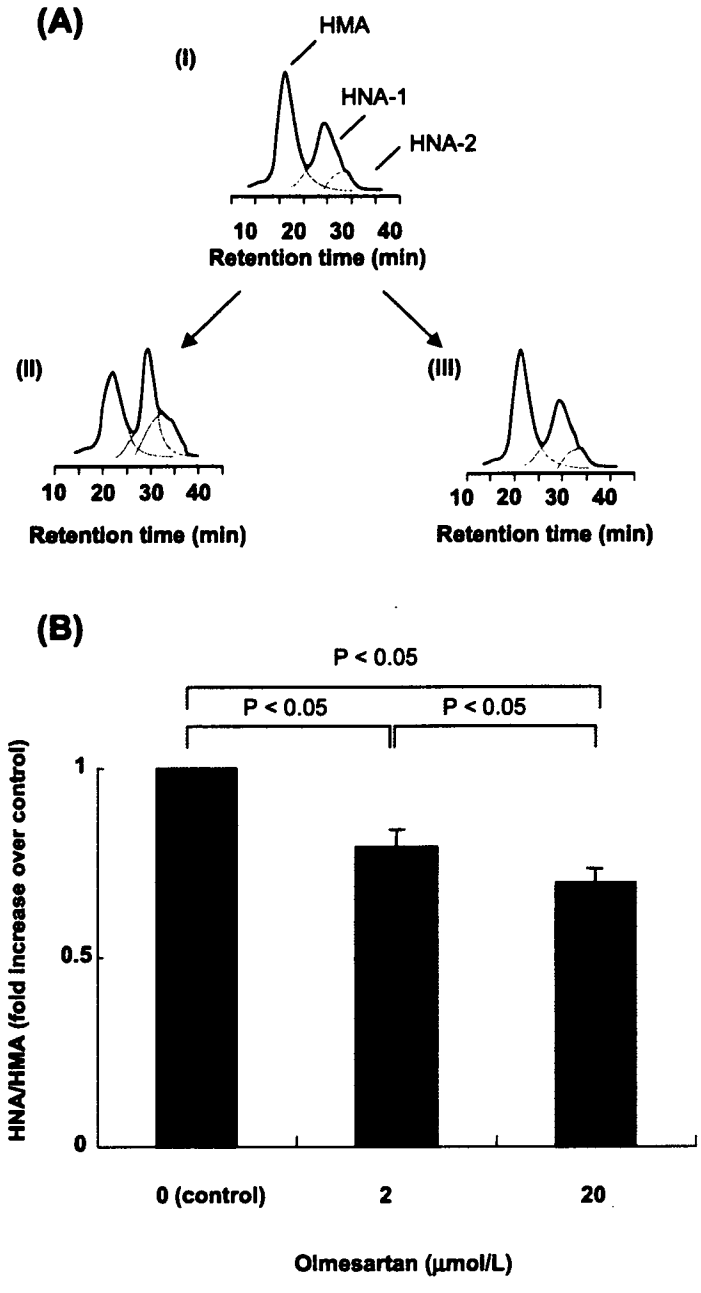

Fig. 1. *A: HPLC profile of in vitro–oxidized serum albumin. HPLC profile of albumin from a uremic subject under control conditions before incubation (I). In II and III, plasma was incubated without or with 20 μmol/L of olmesartan for 7 days. HMA, mercaptalbumin (reduced form); HNA-1, nonmercaptalbumin (disulfide form); HNA-2, nonmercaptalbumin (oxidized form). B: Effect of olmesartan on the HPLC profiles of serum albumin. The calculated ratio of oxidized to reduced albumin ([HNA-1+HNA-2]/[HMA]). Values are expressed as the fold-increase over the control (without olmesartan) (mean±SEM).*

room temperature for 30 min, absorbances were measured at 560 nm and converted to concentrations using the molar absorption coefficient of 3.70×10^4 mol/L/cm (*17*).

Antioxidant Activity of Olmesartan *In Vivo*

Individual Plasma Carbonyl Contents Measurement

The oxidation of individual plasma proteins was measured by Western blot analysis as described by Shacter *et al.* (*20*). Plasma was diluted to 2 mg/mL of total protein with phosphate-buffered saline (PBS) and derivatized with anti-2,4-

dinitrophenylhydrazine (DNP) using an OxyBlot Kit (Serologicals Corporation, Norcross, USA). Samples were diluted to 1 mg/mL of total protein by the addition of an equal volume of nonreducing sample buffer, and 15 μL samples were electrophoresed on duplicate SDS-PAGE gels. Following electrotransfer to a PVDF membrane, one blot was stained for DNP using the OxyBlot Kit reagents. The second blot was stained with Coomassie brilliant blue G for proteins. The bands were visualized with chemiluminescent chemicals and captured on film at 10 min. Each Western blot included samples from both HD patients and healthy controls. These data were recorded as DNP area/protein area, and are reported as densitometry units. The means for each subject group are calculated from each blot.

Statistics

Statistical significance was evaluated by the 2-tailed paired Student's *t*-test for comparison between 2 mean values and by ANOVA followed by the Newman-Keuls test for comparison among >2 mean values. For all analyses, $p<0.05$ was regarded as being statistically significant. The results are reported as the mean±SEM.

Results

Inhibition of Oxidized Albumin Formation by Olmesartan

We determined the HPLC profile of serum albumin with or without olmesartan before and after the *in vitro* incubation. The HPLC profile of plasma for mercaptalbumin (HMA) and nonmercaptalbumin-1 and -2 (HNA-1 and HNA-2) in uremic patients before incubation is shown in Fig. 1A (I). One week after the incubation, in the absence of olmesartan, HMA was reduced and both the HNA-1 and HNA-2 fractions were further increased (Fig. 1A (II)). In the presence of olmesartan, the oxidation of albumin was decreased (Fig. 1A (III)). The ratio of the HNA fraction (HNA-1 and HNA-2) to the HMA fraction was calculated and the results are summarized in Fig. 1B. Treatment with olmesartan caused a significant decrease (21.7±4.1%) in the HNA/HMA ratio at 2 μmol/L of olmesartan ($p<0.05$ *vs.* control), with a further reduction (31.2±3.7%) at 20 μmol/L of olmesartan. These results demonstrate that olmesartan inhibits the oxidation of serum albumin in a concentration-dependent manner.

Inhibition of Albumin Hydroperoxides Formation by Olmesartan

The ability of olmesartan to inhibit the generation of protein hydroperoxides by hydroxyl radicals was measured by irradiating HSA with or without olmesartan by a γ-source, followed by an assay for hydroperoxides. The results showed that olmesartan lowered the amount of HSA hydroperoxides generated and that the effect was concentration- and time-dependent (Fig. 2). These results are consistent with albumin oxidation being inhibited by olmesartan, as shown in Fig. 1.

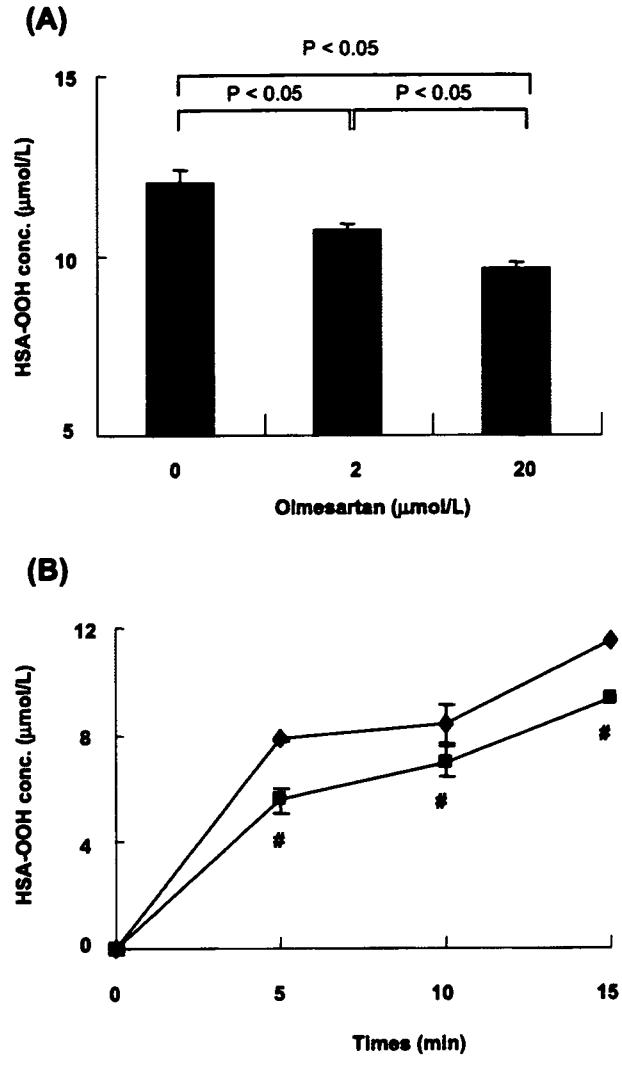

Fig. 2. *Effect of the presence of olmesartan on HSA-OOH formation after γ-irradiation. Concentration (A)- and time (B)- dependent formation of HSA-OOH with olmesartan (20 μmol/L) (■) and with olmesartan (2 μmol/L) (◆). The concentration of HSA was 20 μmol/L and the cobalt-60 radiation dose rate was 36 Gy/min. Hydroperoxide concentrations were measured using the perchloric acid–xylenol orange assay method. Each bar represents the mean±SEM from triplicate samples. HSA-OOH, human serum albumin hydroperoxide. #$p<0.05$ vs. 2 μmol/L olmesartan.*

Carbonylation of Plasma Protein from HD Patients with or without Olmesartan

We also investigated the antioxidant effects of olmesartan *in vivo*. As shown in Fig. 3, oxidized proteins were derivatized

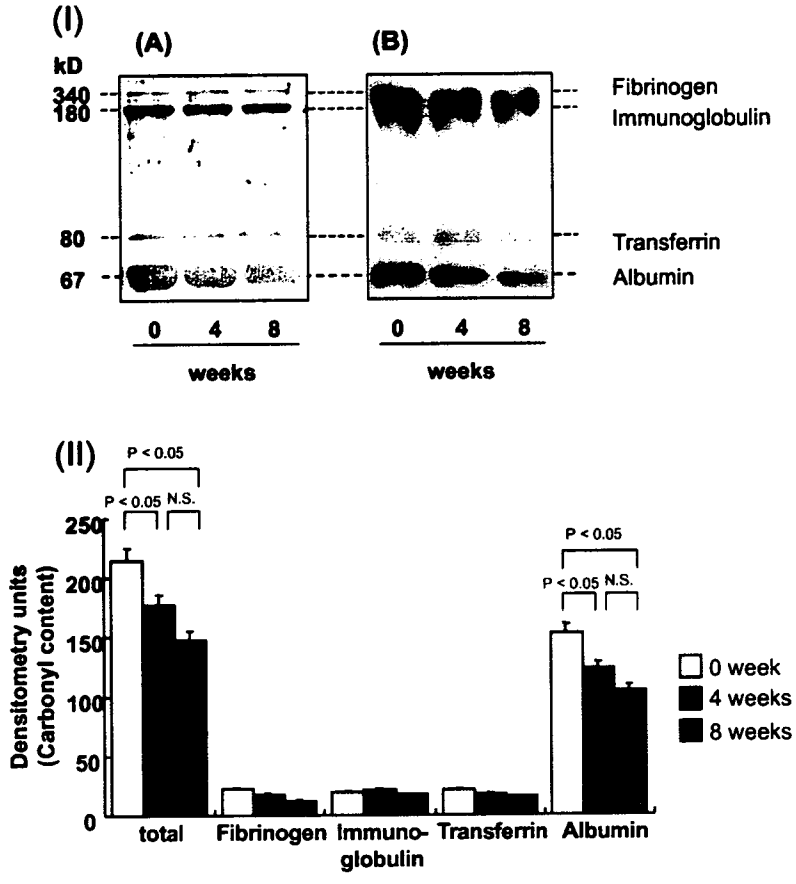

Fig. 3. *Carbonyl content of major plasma proteins from HD patients treated with olmesartan at different times. (I) Plasma samples from HD patients with or without olmesartan were derivatized with DNP after 4 and 8 weeks of treatment and subjected to duplicate SDS-PAGE gels. Following electrotransfer, one blot was stained with Coomassie brilliant blue G for protein (A) and the second blot was stained for DNP using OxiBlot kit reagents (B). (II) Carbonyl formation of major plasma proteins (albumin, transferrin, immunoglobulin, and fibrinogen) was determined as the densitometry ratio of the DNP area and the protein area, and is reported in densitometry units. Values are expressed as the mean±SEM; n = 6 patients per group.*

with DNP, separated by SDS-gel electrophoresis, and screened with antibodies against dinitrophenyl groups. HSA was the only major plasma protein that was significantly oxidized in HD patients without olmesartan and, in the group treated with the drug, the oxidation of HSA was decreased. There was no significant difference in the carbonyl contents of the other plasma proteins (transferrin, immunoglobulin, and fibrinogen). These findings show that the decrease in plasma protein carbonyl contents in HD patients was largely due to a decrease in the level of oxidized HSA. Therefore, it would be expected that characterization of the oxidation status of serum albumin might provide useful information regarding the redox state of the human body, prompting us to examine the effect of olmesartan on the oxidation of albumin.

Oxidation of HSA from HD Patients with or without Olmesartan

The ratio of each HSA fraction to total HSA (f[HMA], f[HNA-1], and f[HNA-2]) was calculated and the results are summarized in Fig. 4. Treatment with olmesartan caused a significant decrease (20.5±3.3%) in the HNA/HMA ratio at 4 weeks ($p<0.05$ *vs.* ratio at 0 weeks), and this effect was maintained up to 8 weeks.

BPM Profile from HD Patients with or without Olmesartan

We investigated the mean BPM profiles (systolic blood pressure [SBP] and diastolic blood pressure [DBP]) after 0, 4, and 8 weeks of treatment with olmesartan. Olmesartan therapy significantly reduced the SBP and DBP at 8 weeks *vs.* the baseline ($p<0.05$) (data not shown). These findings strongly

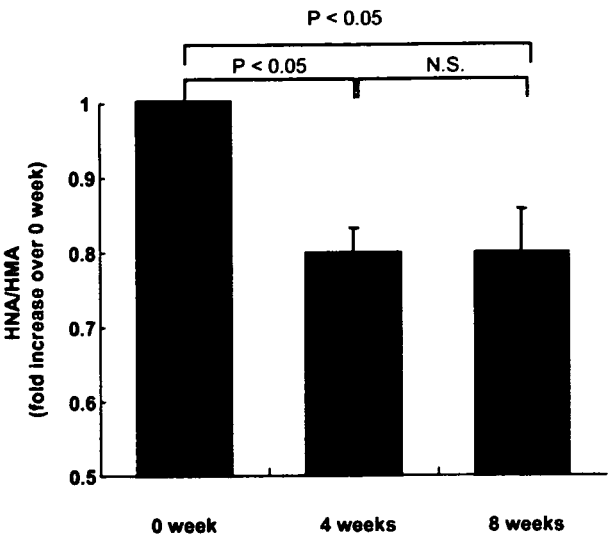

Fig. 4. *Effect of olmesartan on HPLC profiles of serum albumin in vivo. Aliquots (5 μL) of serum were obtained at 0, 4, and 8 weeks after the start of olmesartan therapy and subjected to HPLC using a Shodex Asahipak ES-502N column. The ratio of oxidized albumin to reduced albumin was then calculated ([HNA-1+HNA-2]/[HMA]). Values are expressed as the fold-increase over the control (0 week) (mean±SEM).*

suggest that olmesartan has a significant long-acting BP-lowering effect in HD patients at a daily dose of 40 mg and that ≥8 weeks are required to reach the maximum antihypertensive effect. Olmesartan levels were not significantly different during the experimental periods, suggesting that olmesartan did not accumulate in HD patients when administered at a dose of 40 mg daily for 8 weeks (data not shown). These results indicate that, although the maximum antihypertensive effect was reached at 8 weeks, treatment with olmesartan caused a significant decrease (20.5±3.3%) in oxidative stress at 4 weeks. Thus, this effect might result in benefits by the clinical use of olmesartan.

Discussion

Oxidative stress has long been incriminated in the development of dialysis complications, such as β_2-microglobulin amyloid arthropathy and the acceleration of atherosclerosis (*21*). Until recently, direct evidence for *in vivo* oxidative stress in HD patients was almost entirely limited to the measurement of lipid peroxidation by-products such as malondialdehyde and other thiobarbituric acid–reactive substances (*22*). Despite the observation that proteins are highly susceptible to oxidative stress, there have been few reports of the production of oxidatively modified proteins in HD procedures. Measurement of markers of protein oxidation such as advanced oxidation protein products and carbonyl content have recently been performed to assess oxidative stress under pathological conditions (*23–26*). In 2001, Himmelfarb *et al.* (*27*) reported that the oxidation of albumin accounts for almost all of the excess plasma protein oxidation in uremic patients as demonstrated by SDS-PAGE and an immunoassay using a DNP antibody. In this study, we showed that the decrease in plasma protein carbonyl content in HD patients was largely due to a decrease in the level of oxidized albumin, and that olmesartan substantially decreased the plasma protein carbonyl content by oxidizing albumin (Fig. 3). Given the fact that, in extracellular fluids, serum albumin plays a major antioxidant role (*28, 29*), we expected that characterization of the oxidation status of serum albumin might provide useful information regarding the redox state of the human body, prompting us to examine the effect of olmesartan on the oxidation of albumin *in vivo*. Previously we reported that purified albumin from HD patients triggered oxidative bursts in neutrophils, and thus appeared to act as a true inflammatory mediator (*30*). Furthermore, the binding of ligands to albumins was found to decrease by oxidative modification of albumin (*25, 30*). Therefore, management of the oxidation status of serum albumin is an important issue in cases of CKD and medicine therapy.

Serum albumin can be separated into HMA and HNA by HPLC (*31*) and is used to determine the redox state under various pathophysiological conditions (*32–35*). We also recently demonstrated by HPLC that serum albumin shows high levels of oxidation in HD patients compared with age- and gender-matched healthy subjects, and that HPLC analysis of serum albumin can be useful for the quantitative and qualitative evaluation of oxidative stress in HD patients (*16*). However, until the present study, HPLC analysis of serum albumin had not been used to determine whether the antioxidant activity of olmesartan is expressed in *in vivo* and *in vitro* systems.

In a previous study, Miyata *et al.* (*15*) also had suggested that the antagonist olmesartan inhibited the formation of two AGE, pentosidine and carboxymethyllysine, during incubation with uremic plasma or bovine serum albumin. This effect is unlike that of the calcium channel blocker nifedipine. These results suggest that olmesartan has antioxidant activity in HD patients. However, they applied a relatively higher concentration of olmesartan (mmol/L order) to demonstrate the antioxidant effects. Therefore, the anti-oxidant effects of olmesartan at a clinical concentration (around 2 μmol/L) remain to be determined. In the present study, using a highly sensitive HPLC method, a clinical concentration of olmesartan (0–20 μmol/L) was found to attenuate the oxidized albumin ratio *in vitro* based on the redox states of Cys-34 of albumin (Fig. 1) (*36, 37*). We also examined the possibility that olmesartan can inhibit such damage by preventing the formation of protein peroxides or by decreasing any peroxide groups that are generated by the radicals. The tests showed that irradiated olmesartan did not form stable peroxides (data not shown). However, when HSA (20 μmol/L) was exposed to radiation-generated hydroxyl radicals in the presence of 2.0 or 20 μmol/L of olmesartan, the HSA damage was inhibited, as evidenced

by the amounts of peroxides generated (Fig. 2). These findings suggest that olmesartan, at a clinical concentration, protects HSA against the general oxidation caused by hydroxyl radicals. In fact, olmesartan is a biphenyl tetrazole derivative and its common core structure, 5-(4′-methylbiphenyl-2-yl)-1H-tetrazol, is thus probably responsible for the inhibitory effect on oxidative stress (*15*). This structure is also important for binding to AT1 receptors and is one of the active sites of the inverse agonist. Furthermore, the imidazole ring of olmesartan has carboxyl and hydroxyl groups different from those in other ARBs, which may be the reason for its potent inverse agonist activity.

The findings of our *in vivo* study clearly demonstrated that olmesartan caused a decrease in the levels of oxidized albumin in HD patients after 4 weeks of treatment and this effect was maintained until 8 weeks (Fig. 4), while olmesartan therapy significantly reduced SBP and DBP at 8 weeks (data not shown). Therefore, these results suggest that olmesartan not only reduces SBP but also reduces oxidative stress. Angiotensin II plays an important role in increasing BP by stimulating AT1 receptors. To prevent angiotensin II from acting, ARBs block the binding of angiotensin II to AT1 receptors. Since ARBs block the effects of angiotensin II, they might be expected to decrease the risk of coronary artery disease, cardiac failure, renal dysfunction, and cerebral artery diseases (*38*). Some studies have shown that ARBs do, in fact, significantly reduce these risks, and that their mechanisms of action may involve the blocking of angiotensin II–related functions, such as inducing the production of growth factors and cytokines, in addition to their hypotensive effect. Moreover, angiotensin II has been reported to modulate NADPH oxidase activity in a number of studies, and aldosterone has also been implicated in the generation of reactive oxygen species (*7*, *39*, 40). In theory, then, blocking of the RAAS by ARBs should be effective for reducing oxidative stress. In this work, we showed that olmesartan exhibited antioxidant activity *in vivo*, but this activity might have been a combination of direct and indirect antioxidant effects, such as modulation of NADPH oxidase activity. Moreover, various factors in addition to the above effects may play a role in the antioxidant activity of olmesartan. Therefore, determining the mechanism by which olmesartan decreases the ROS production will require further *in vitro* and *in vivo* studies.

We recently demonstrated that telmisartan effectively lowered the extent of BP and reduced oxidative stress and that it is safe and well-tolerated by HD patients (*17*). Interestingly, the reduction of oxidative stress by olmesartan was slightly higher than that by telmisartan. This effect might have been due to its structure and strong binding to AT1 receptors. However, a long-term study in a large population is required to elucidate the influence of olmesartan therapy on CVD mortality and morbidity in HD patients.

In summary, olmesartan effectively lowered the extent of oxidative damage to HSA in *in vitro* and *in vivo* studies, and this effect might confer benefits beyond simple BP reduction.

Acknowledgements

We wish to thank the Sankyo Pharmaceutical (Tokyo, Japan) for the generous gift of olmesartan.

References

1. Suzuki H: Treatment of hypertension in chronic renal insufficiency. *Intern Med* 2000; **39**: 773–777.
2. Suzuki H: Angiotensin type 1 receptor blockers in chronic kidney disease. *Contrib Nephrol* 2004; **143**: 159–166.
3. Okada K, Hirano T, Ran J, Adachi M: Olmesartan medoxomil, an angiotensin II receptor blocker ameliorates insulin resistance and decreases triglyceride production in fructose-fed rats. *Hypertens Res* 2004; **27**: 293–299.
4. Mizuno M, Sada T, Kato M, Koike H: Renoprotective effects of blockade of angiotensin II AT1 receptors in an animal model of type 2 diabetes. *Hypertens Res* 2002; **25**: 271–278.
5. Martina B, Dieterle T, Sigle JP, Surber C, Battegay E: Effects of telmisartan and losartan on left ventricular mass in mild-to-moderate hypertension. A randomized, double-blind trial. *Cardiology* 2003; **99**: 169–170.
6. Koh KK, Ahn JY, Han SH, *et al*: Pleiotropic effects of angiotensin II receptor blocker in hypertensive patients. *J Am Coll Cardiol* 2003; **42**: 905–910.
7. Griendling KK, Minieri CA, Ollerenshaw JD, Alexander RW: Angiotensin II stimulates NADH and NADPH oxidase activity in cultured vascular smooth muscle cells. *Circ Res* 1994; **74**: 1141–1148.
8. Ruiz-Ortega M, Lorenzo O, Ruperez M, Konig S, Wittig B, Egido J: Angiotensin II activates nuclear transcription factor κB through AT1 and AT2 in vascular smooth muscle cells: molecular mechanisms. *Circ Res* 2000; **86**: 1266–1272.
9. Tschudi MR, Mesaros S, Luscher TF, Malinski T: Direct *in situ* measurement of nitric oxide in mesenteric resistance arteries: increased decomposition by superoxide in hypertension. *Hypertension* 1996; **27**: 32–35.
10. Weiss D, Kools JJ, Taylor WR: Angiotensin II–induced hypertension accelerates the development of atherosclerosis in ApoE-deficient mice. *Circulation* 2001; **103**: 448–454.
11. Haller H, Viberti GC, Mimran A, *et al*: Preventing microalbuminuria in patients with diabetes: rationale and design of the Randomised Olmesartan and Diabetes Microalbuminuria Prevention (ROADMAP) study. *J Hypertens* 2006; **24**: 403–408.
12. Yamaguchi K, Ura N, Murakami H, *et al*: Olmesartan ameliorates insulin sensitivity by modulating tumor necrosis factor-alpha and cyclic AMP in skeletal muscle. *Hypertens Res* 2005; **28**: 773–778.
13. Izuhara Y, Nangaku M, Inagi R, *et al*: Renoprotective properties of angiotensin receptor blockers beyond blood pressure lowering. *J Am Soc Nephrol* 2005; **16**: 3631–3641.
14. Yuan Z, Nimata M, Okabe TA, *et al*: Olmesartan, a novel AT1 antagonist, suppresses cytotoxic myocardial injury in autoimmune heart failure. *Am J Physiol Heart Circ Physiol* 2005; **289**: H1147–H1152.
15. Miyata T, van Ypersele de Strihou C, Ueda Y, *et al*: Angio-

tensin II receptor antagonists and angiotensin-converting enzyme inhibitors lower *in vitro* the formation of advanced glycation end products: biochemical mechanisms. *J Am Soc Nephrol* 2002; **13**: 2478–2487.
16. Anraku M, Kitamura K, Shinohara A, *et al*: Intravenous iron administration induces oxidation of serum albumin in hemodialysis patients. *Kidney Int* 2004; **66**: 841–848.
17. Shimada H, Kitamura K, Anraku M, *et al*: Effect of telmisartan on ambulatory blood pressure monitoring, plasma brain natriuretic peptide, and oxidative status of serum albumin in hemodialysis patients. *Hypertens Res* 2005; **28**: 987–994.
18. Mera K, Anraku M, Kitamura K, *et al*: Oxidation and carboxy methyl lysine-modification of albumin: possible involvement in the progression of oxidative stress in hemodialysis patients. *Hypertens Res* 2005; **28**: 973–980.
19. Gay CA, Gebicki JM: Measurement of protein and lipid hydroperoxides in biological systems by the ferric-xylenol orange method. *Anal Biochem* 2003; **315**: 29–35.
20. Shacter E, Williams JA, Lim M, Levine RL: Differential susceptibility of plasma proteins to oxidative modification: examination by western blot immunoassay. *Free Radic Biol Med* 1994; **17**: 429–437.
21. Descamps-Latscha B, Witko-Sarsat V: Importance of oxidatively modified proteins in chronic renal failure. *Kidney Int* 2001; **59** (Suppl 78): S108–S113.
22. Daschner M, Lenhartz H, Botticher D, *et al*: Influence of dialysis on plasma lipid peroxidation products and antioxidant levels. *Kidney Int* 1996; **50**: 1268–1272.
23. Witko-Sarsat V, Gausson V, Nguyen AT, *et al*: AOPP-induced activation of human neutrophil and monocyte oxidative metabolism: a potential target for *N*-acetylcysteine treatment in dialysis patients. *Kidney Int* 2003; **64**: 82–91.
24. Witko-Sarsat V, Gausson V, Descamps-Latscha B: Are advanced oxidation protein products potential uremic toxins? *Kidney Int* 2003; **63** (Suppl 84): S11–S14.
25. Witko-Sarsat V, Friedlander M, Capeillere-Blandin C, *et al*: Advanced oxidation protein products as a novel marker of oxidative stress in uremia. *Kidney Int* 1996; **49**: 1304–1313.
26. Odetti P, Garibaldi S, Gurreri G, Aragno I, Dapino D: Protein oxidation in hemodialysis and kidney transplantation. *Metabolism* 1996; **45**: 1319–1322.
27. Himmelfarb J, McMonagle E: Albumin is the major plasma protein target of oxidant stress in uremia. *Kidney Int* 2001; **60**: 358–363.
28. Bourdon E, Loreau N, Blache D: Glucose and free radicals impair the antioxidant properties of serum albumin. *FASEB J* 1999; **13**: 233–244.
29. Gebicki JM: Protein hydroperoxides as new reactive oxygen species. *Redox Rep* 1997; **3**: 99–110.
30. Mera K, Anraku M, Kitamura K, Nakajou K, Maruyama T, Otagiri M: The structure and function of oxidized albumin in hemodialysis patients: its role in elevated oxidative stress *via* neutrophil burst. *Biochem Biophys Res Commun* 2005; **334**: 1322–1338.
31. Sogami M, Nagaoka S, Era S, Honda M, Noguchi K: Resolution of human mercapt- and nonmercaptalbumin by high-performance liquid chromatography. *Int J Pept Protein Res* 1984; **24**: 96–103.
32. Hayakawa A, Kuwata K, Era S, *et al*: Alteration of redox state of human serum albumin in patients under anesthesia and invasive surgery. *J Chromatogr B Biomed Sci Appl* 1997; **698**: 27–33.
33. Sogami M, Era S, Nagaoka S, *et al*: High-performance liquid chromatographic studies on non-mercapt in equilibrium with mercapt conversion of human serum albumin. *J Chromatogr* 1985; **332**: 19–27.
34. Suzuki E, Yasuda K, Takeda N, *et al*: Increased oxidized form of human serum albumin in patients with diabetes mellitus. *Diabetes Res Clin Pract* 1992; **18**: 153–158.
35. Soejima A, Kaneda F, Manno S, *et al*: Useful markers for detecting decreased serum antioxidant activity in hemodialysis patients. *Am J Kidney Dis* 2002; **39**: 1040–1046.
36. Soriani M, Pietraforte D, Minetti M: Antioxidant potential of anaerobic human plasma: role of serum albumin and thiols as scavengers of carbon radicals. *Arch Biochem Biophys* 1994; **312**: 180–188.
37. Stamler JS, Simon DI, Osborne JA, *et al*: *S*-Nitrosylation of proteins with nitric oxide: synthesis and characterization of biologically active compounds. *Proc Natl Acad Sci U S A* 1992; **89**: 444–448.
38. Unger T, Culman J, Gohlke P: Angiotensin II receptor blockade and end-organ protection: pharmacological rationale and evidence. *J Hypertens Suppl* 1998; **16**: S3–S9.
39. Rajagopalan S, Duquaine D, King S, Pitt B, Patel P: Mineralocorticoid receptor antagonism in experimental atherosclerosis. *Circulation* 2002; **105**: 2212–2216.
40. Yao L, Kobori H, Rahman M, *et al*: Olmesartan improves endothelin-induced hypertension and oxidative stress in rats. *Hypertens Res* 2004; **27**: 493–500.

0090-9556/08/3601-81–86$20.00
DRUG METABOLISM AND DISPOSITION

DMD 36:81–86, 2008

Vol. 36, No. 1
16873/3285340
Printed in U.S.A.

Subdomain IIIA of Dog Albumin Contains a Binding Site Similar to Site II of Human Albumin

Ken-ichi Kaneko, Hikaru Fukuda, Victor Tuan Giam Chuang, Keishi Yamasaki, Kohichi Kawahara, Hitoshi Nakayama, Ayaka Suenaga, Toru Maruyama, and Masaki Otagiri

Graduate School of Pharmaceutical Sciences, Kumamoto University, Kumamoto, Japan (K.K., H.F., K.K., H.N., A.S., T.M., M.O.); School of Pharmacy, Curtin University of Technology, Perth, Western Australia, Australia (V.T.G.C.); and Graduate School of Pharmaceutical Sciences, Sojo University, Kumamoto, Japan (K.Y.)

Received May 25, 2007; accepted October 4, 2007

ABSTRACT:

Dog albumin contains a specific drug-binding site that binds most of the site II ligands of human albumin. This study was undertaken to elucidate the structural configuration of this binding site using a photoaffinity labeling technique. Dog albumin and albumins of other animal species were photolabeled with [^{14}C]ketoprofen. The photolabeled albumins were cleaved with cyanogen bromide (CNBr) and analyzed autoradiographically after electrophoretic separation. A 11.6-kDa CNBr fragment of the photolabeled dog albumin was found to have incorporated most of the radioactivity. Site II ligands of human albumin inhibited photoincorporation of radioactivity to this fragment. The binding constants of human and dog albumins ranged from 10 to 12 × 10^5 M^{-1}, at least twice as high as those of rat, rabbit, and bovine albumins. Edman degradation was performed to elucidate the amino acid sequence of the photolabeled peptide derived from further digestion of the dog 11.6-kDa CNBr fragment with lysyl endopeptidase. The sequence was XXSESLVXRX, which corresponds to Cys^{476}-Arg^{485} of dog albumin. Dog albumin contains a binding site that may have a binding microenvironment similar to that of site II on human albumin. Therefore, dog may be a better experimental animal for data extrapolation from animal to human with regard to site II drug-drug interactions.

The binding of drugs in human plasma, in most cases, is caused mainly by binding to albumin because albumin is normally present at high concentrations of approximately 40 mg/ml (0.6 mM) in healthy human subjects (Peters, 1996; Davi et al., 1999) and also by the presence of high-affinity binding sites in the protein. In some cases, albumin binding will influence the pharmacodynamic activity of the drug also (Lewis et al., 2006). Determination of the distribution and plasma protein binding of a drug for species used in preclinical safety investigations and characterization of the interaction of the drug with human albumin can be critical for its pharmacokinetics and are needed for a comparison of pharmacokinetics across species (Kosa et al., 1997; Weiss et al., 2006). Research on species differences in albumin binding of drugs has been done, but in most cases only the binding characteristics were investigated, with very few studies on the binding sites of albumins of different species (Mizojiri et al., 1997; Nonaka et al., 2003; Acharya et al., 2006). Hence, elucidation of the drug-binding sites on albumins of different species will provide useful information when drug interactions with animal models are investigated.

Albumins bind endogenous as well as exogenous substances including drugs (Peters, 1996; Petersen et al., 2002; Simard et al., 2006). There are at least two discrete drug-binding sites on human albumin, namely, site I and site II, according to the classification of Sudlow et al. (1975). Crystallographic analysis of human albumin confirms the locations of the two binding sites I and II at domains II and III, respectively (Petitpas et al., 2003; Ghuman et al., 2005). We have previously reported that rat, rabbit, and bovine albumins contain a binding site similar to site I of human albumin, whereas dog albumin contains a binding site similar to site II of human albumin using ibuprofen and diazepam as the site II probes (Kosa et al., 1997). However, the conclusion was made on the basis of the results of a fluorescent probe displacement experiment, which did not address the location of binding sites on the protein molecule. In addition, at present only crystallographic structures of human and horse albumins are available (Ho et al., 1993; Curry et al., 1998). The lack of structural data for albumins of other animal species has, to a certain extent, impeded further assessment of drug-binding models.

In a previous study, we had successfully identified the binding site of ketoprofen (KP) on human albumin. KP is a site II ligand of human albumin that can be used as a labeling agent because of its benzophenone moiety. In that study, the binding site structural configuration of site II of human albumin was found to consist of Cys^{476}-Pro^{499} which forms part of subdomain IIIA of human albumin (Chuang et al., 1999). Hence, to identify the location of the KP binding site on dog albumin, [^{14}C]KP was used to photolabel dog albumin and the amino acid sequence of the photolabeled dog albumin peptide was determined.

Article, publication date, and citation information can be found at http://dmd.aspetjournals.org.
doi:10.1124/dmd.107.016873.

ABBREVIATIONS: KP, ketoprofen; PAGE, polyacrylamide gel electrophoresis; CNBr, cyanogen bromide; TFA, trifluoroacetic acid; WF, warfarin; OCT, sodium octanoate; DZP, diazepam; IP, ibuprofen; HPLC, high-performance liquid chromatography; Lys-C, lysyl endopeptidase; PVDF, polyvinylidene diflouride; CD, circular dichroism; HSA, human serum albumin; UCN-01, 7-hydroxystaurosporine.

Materials and Methods

Materials. Human, dog, rat, rabbit, and bovine albumins were obtained from Sigma-Aldrich (St. Louis, MO). Before all experiments, all albumins were defatted with activated charcoal in solution at 4°C, acidified with HCl to pH 3 and then lyophilized. The albumins used in this study showed only one band of approximately 66 kDa in SDS-PAGE. [^{14}C]KP (12.95 μCi/mmol) was obtained from Hisamitsu Pharmaceutical Co., Inc., Tosu Laboratories (Saga, Japan). Cyanogen bromide (CNBr), dithiothreitol, and trifluoroacetic acid (TFA) were obtained from Nacalai Tesque (Kyoto, Japan). Warfarin (WF) was obtained from Eisai Co., Ltd. (Tokyo, Japan). Sodium octanoate (OCT) was obtained from Wako Pure Chemical Industries, Ltd. (Osaka, Japan). Diazepam (DZP) was obtained from Sumitomo Pharmaceuticals Co., Ltd. (Osaka, Japan). Ibuprofen (IP) was obtained from Kaken Pharmaceutical Co., Ltd. (Tokyo, Japan). All other chemicals were of analytical grade.

Photoaffinity Labeling of Albumins with [^{14}C]KP. Albumin (50 μM) was incubated with [^{14}C]KP (25 μM) in the absence and presence of WF, IP, OCT, and DZP (250 μM), in 100 μl of 20 mM Tris buffer, at pH 7.4 in a 1.5-ml Eppendorf tube at room temperature in the dark for 60 min. The incubation mixture was then placed on ice and irradiated for 30 min at a wavelength of longer than 320 nm by a 100-W black light/blue lamp (Ultra-Violet Products, Inc., San Gabriel, CA) at a distance of 10 cm. After irradiation, the photolabeled albumins were precipitated by adding 1 ml of acetone, followed by centrifugation at 15,000 rpm for 10 min. The pellet was reductively pyridylethylated.

Reductive Pyridylethylation. One hundred microliters of the reduction medium (6 M guanidinium HCl, 1 M Tris buffer, pH 8.0, 20 mM EDTA, and 100 mM dithiothreitol) was added to the pellet, which was then incubated under N_2 at 37°C for at least 12 h. After the addition of 1 μl of 4-vinylpyridine, the mixture was incubated under N_2 for an additional 30 min at room temperature in the dark. At the end of the pyridylethylation reaction, 1 ml of acetone and 100 μl of 0.1% TFA was added to the mixture to terminate the reaction. The suspension was then vortexed vigorously followed by a light centrifugation. One milliliter of ethanol was added, the mixture was further vortexed to remove the salts and unreacted 4-vinylpyridine, and the suspension was centrifuged at 15,000 rpm for 10 min.

CNBr Cleavage and Tricine SDS-PAGE. The pyridylethylated pellet was dissolved in 100 μl of CNBr in 70% formic acid (CNBr-methionine residues = 200:1) and incubated under N_2 for 24 h in the dark at room temperature. 1 ml of Milli-Q water was added at the end of the CNBr cleavage to stop the reaction, and the resulting mixture was lyophilized. The lyophilized CNBr fragments were resuspended in 100 μl of 0.1% TFA, and the protein concentration was determined by a Bradford assay in which 6.5 μg of the fragment mixture was applied to each lane of the gel with separation using Tricine SDS-PAGE.

Autoradiographic Analysis. For autoradiographic analysis, the dried SDS-PAGE gel was placed in contact with an imaging plate (BAS III; Fuji Film Co., Tokyo, Japan) in a cassette (BAS cassette 2040; Fuji Film Co.) at room temperature for 48 h. The imaging plate was scanned and analyzed using a Bio-Imaging Analyzer (model BAS FLA-3000 G; Fuji Film Co.) and was then analyzed using L Process V 1.6 software (Fuji Film Science Lab 98; Fuji Film Co.). The incorporation of radioactivity into individual fragments was quantified using Image Gauge V 3.1 software (Fuji Film Co.).

Capillary HPLC Separation and Sequence Analysis. The 11.6-kDa CNBr peptide of dog albumin was eluted from the gel after Tricine SDS-PAGE with an Electro-Eluter (model 422; Bio-Rad, Hercules, CA). The peptide was then digested with the enzyme lysyl endopeptidase (Lys-C) in 20 mM ammonium bicarbonate at 37°C for 16 h. Ten microliters of the digestion sample was then injected onto the ABI 173 A MicroBlotter Capillary HPLC System (PerkinElmer Life and Analytical Sciences, Waltham, MA). The sample was manipulated following the manufacturer's instructions. The blotted membrane from the capillary HPLC separation was in contact with an imaging plate for 48 h before autoradiographic analysis. The PVDF membrane was positioned with the chromatogram of a peptide map from the ABI 173 A MicroBlotter Capillary HPLC System. A portion of the PVDF membrane was excised for sequencing with reference to the autoradiogram. Edman degradation of the photolabeled peptide was carried out with a Procise Sequencer (Applied Biosystems, Foster City, CA).

TABLE 1

Binding parameters of KP to different serum albumins at pH 7.4

Results were determined by ultrafiltration. Values represent the mean ± S.D.

	n_1	K_1 ($\times 10^5$ M^{-1})	n_2	K_2 ($\times 10^4$ M^{-1})
Human	1.34 ± 0.04	10.02 ± 0.47	4.82 ± 0.16	2.11 ± 0.13
Dog	0.91 ± 0.01	11.65 ± 0.21	7.09 ± 0.62	0.66 ± 0.09
Bovine	1.72 ± 0.13	4.62 ± 0.48	5.46 ± 0.59	1.16 ± 0.30
		n	K ($\times 10^5$ M^{-1})	
Rat		3.32 ± 0.05	2.45 ± 0.06	
Rabbit		2.93 ± 0.05	3.20 ± 0.15	

Determination of Binding Parameters. To quantitatively analyze the binding mode, binding parameters were determined by ultrafiltration. Ultrafiltration was performed using Ultrafree MC (Amicon Division, Danvers, MA). Ligands were added to 400 μl of albumins (10 μM) in 20 mM Tris buffer, at pH 7.4, and preincubated at 25°C for 30 min before centrifugation (2000 rpm for 20 min). To determine the free ligand concentrations (C_f), a 200-μl aliquot of the filtrate was added to 2 ml of scintillation cocktail in a scintillation vial (Pyrex; Asahi Techno Glass Corporation, Chiba, Japan), vortexed, and counted by using a scintillation counter (LSC-5121, Aloka Co., Ltd, Tokyo, Japan). No adsorption of the ligands to membrane or apparatus was detectable.

Binding parameters were determined by fitting the experimental data to the following equation using a nonlinear least-squares program (MULTI program):

$$r = \sum_{i=1}^{m} \frac{n_i K_i C_f}{1 + K_i C_f} \quad (1)$$

where n_i is the number of binding sites, K_i is the binding constant in the ith binding class, and r is the moles of bound ligand per mole of total protein (C_b/P_t).

CD Spectra Measurements in the Presense of KP. CD spectra were measured using a JASCO J-820 spectropolarimeter (JASCO, Tokyo, Japan) at 25°C with a 10-mm path length cell. The concentration of various albumins was 60 μM and the KP concentration was 100 μM in 20 mM Tris-HCl buffer (pH 7.4). The scan speed was adjusted at 10 nm/min and was the average of three scans, with the range of wavelength scanned from 300 to 400 nm. The results were represented as observed ellipticity (θ_{obs}) in millidegrees. Induced CD was determined as the CD of the albumin-KP mixture after subtraction of CD of the albumin alone.

Results

Binding Parameters of KP to Albumins of Different Species. The number of binding sites and the corresponding binding constants for binding of KP to albumins were estimated using ultrafiltration (Table 1; Fig. 1). The primary binding constants of human and dog albumins ranged from 10 to 12 $\times$ 10^5 M^{-1}, at least twice as high as those of rat, rabbit, and bovine albumins, which ranged within 2 to 5 $\times$ 10^5 M^{-1}. In human, dog, and bovine albumins, KP binds at primary and secondary sites. On the other hand, in rat and rabbit albumins, KP binds to three sites that could not be categorized into primary or secondary level.

CD Spectra Measurements of Albumins in the Presence of KP. When KP binds to HSA, a specific Cotton effect will be induced (Dubois et al., 1994; Zandomeneghi, 1995). Figure 2 shows the CD spectra obtained when KP was added to the different albumin solutions. Binding of KP to human and dog albumins resulted in a negative Cotton effect, with a maximum at approximately 340 nm. Binding of KP to rabbit albumin led to a decrease in the specific negative Cotton effect compared with those induced in human and dog albumins. Meanwhile, the spectrum of bovine albumin-KP binding was appreciably different from those of human, dog, and rabbit

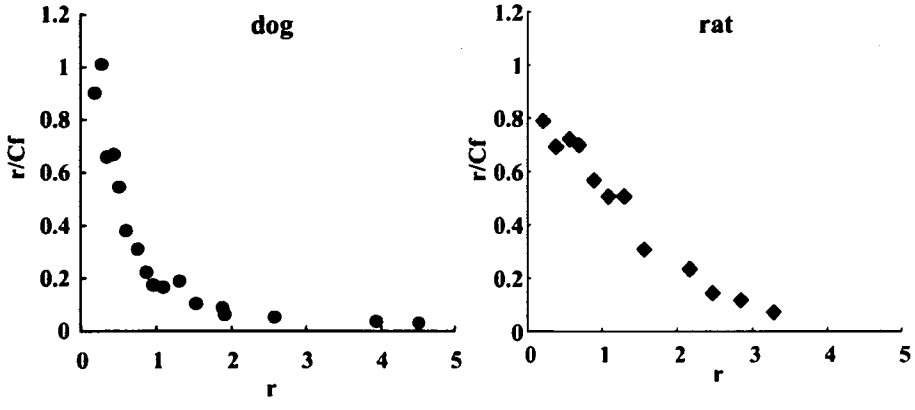

FIG. 1. Scatchard plots of the binding of KP to dog (●) and rat (◆) albumins.

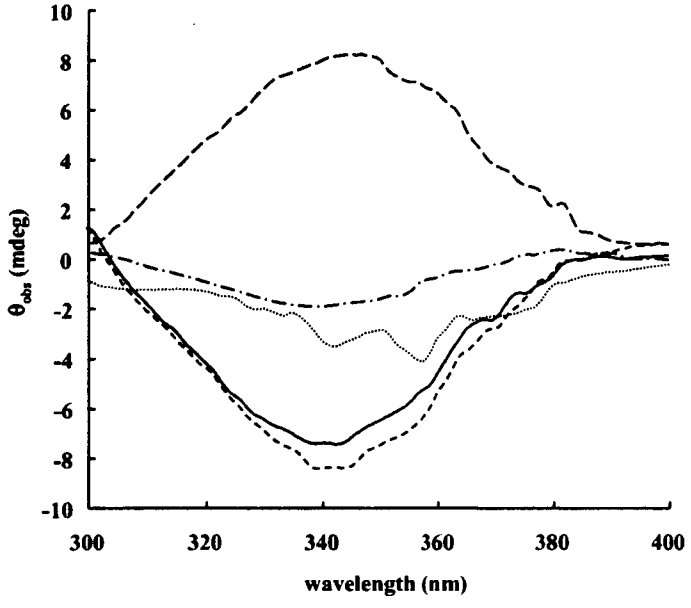

FIG. 2. CD spectra of different albumins in the presence of KP at 25°C. The sample solutions contained 100 μM KP and 60 μM albumin in 20 mM Tris-HCl buffer (pH 7.4). ——, human albumin; ····, dog albumin; - - -, rat albumin; -·-, rabbit albumin; — — —, bovine albumin.

albumins. With an effect different from that of other albumins, binding of KP to rat albumin resulted in a positive Cotton effect.

Photolabeling of Albumins of Various Species with [^{14}C]KP. The autoradiogram in Fig. 3 shows that the radioactivity band appeared only upon photoirradiation of albumins with [^{14}C]KP. Absence of a radioactive band in the samples without irradiation indicated that no covalent attachment of KP to albumin occurred in the dark. Human and dog albumins appeared to incorporate radioactivity to a greater extent than the other albumins.

CNBr Fragments of Albumins of Various Species Photolabeled with [^{14}C]KP. Human and rat albumins have six, whereas dog and bovine albumins contain four methionine residues. Rabbit albumin contains only one methionine residue (Fig. 4). Because the amino acid sequence of each albumin is available, CNBr cleavage products of these albumin can be identified by their mobilities on SDS-containing gels in relation to their molecular weights. Thus, it is possible to preview which subdomain is photolabeled via inspection of the radioactivity intensity of each band (Fig. 5). Significant radioactivity could be observed for the 11.6-kDa CNBr fragments of the photolabeled human and dog albumins and 15.3-kDa bovine albumin was found to have incorporated most of the radioactivity. On the other hand, only a comparatively low level of radioactivity could be ob-

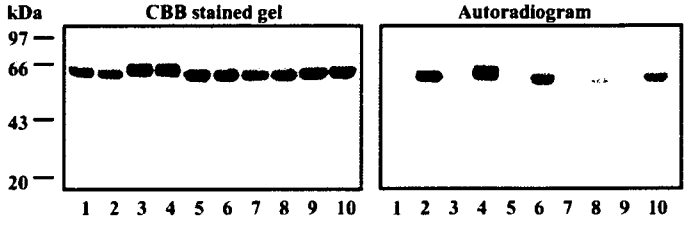

FIG. 3. Photolabeling of different albumins (1, 2, human; 3, 4, dog; 5, 6, rat; 7, 8, rabbit; 9, 10, bovine) with [^{14}C]KP. Lanes 1, 3, 5, 7, and 9, sample taken just before photoirradiation. Lanes 2, 4, 6, 8, and 10, sample taken after 30 min of irradiation

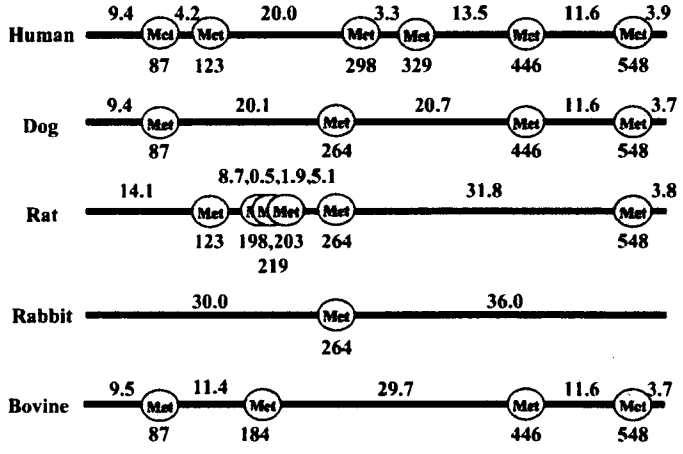

FIG. 4. The position of methionine residues on different albumins. The numbers above the line are calculated molecular weights. The numbers below "Met" are the positions of methionine residues in the amino acid sequence.

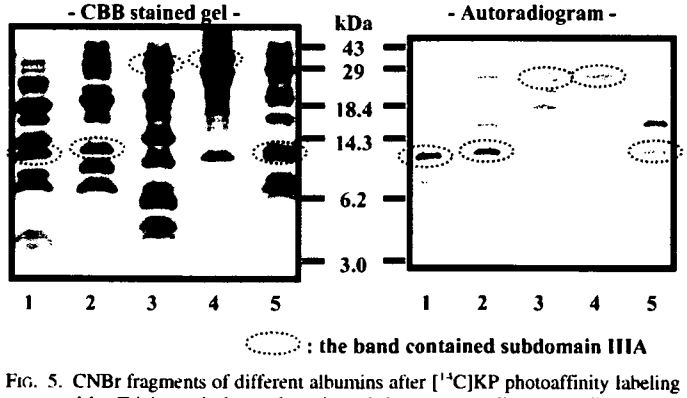

FIG. 5. CNBr fragments of different albumins after [^{14}C]KP photoaffinity labeling separated by Tricine gel electrophoresis and the corresponding autoradiogram. 1, human (11.6 kDa); 2, dog (11.6 kDa); 3, rat (31.8 kDa), 4, rabbit (36.0 kDa), 5, bovine (11.6 kDa).

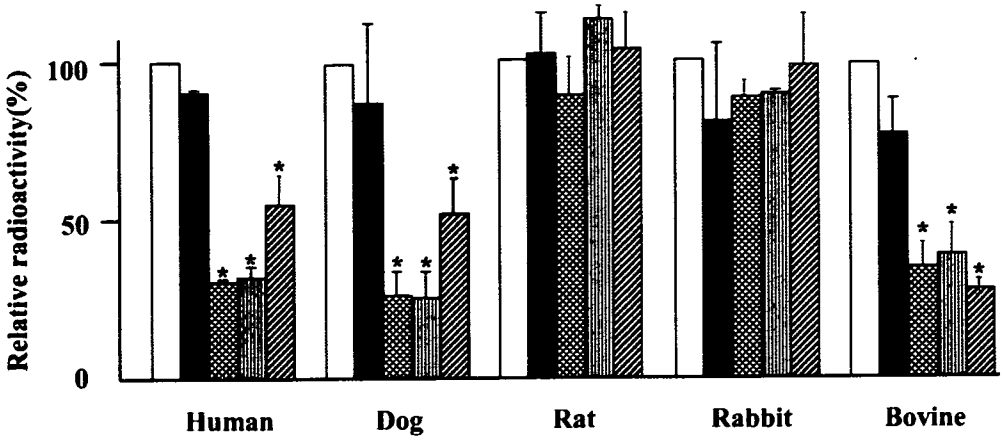

FIG. 6. Autoradiogram and relative radioactivity of the bands containing subdomain IIIA after photoirradiation in the presence of various competitors. The photolabeled albumins were cleaved with CNBr and separated with Tricine gel electrophoresis. The final concentration ratio for different albumins, [^{14}C]KP and competitors was 1:0.5:5. □, control; ■, WF; ■, OCT; □ DZP; and ▨, IP. Data are expressed as means ± S.D. (n = 3–4). *, $p < 0.01$, compared with control.

served for the 31.8-kDa CNBr fragments of the photolabeled rat albumin and 36.0-kDa peptide of rabbit albumin.

Photolabeling Inhibition by Site I and II Ligands of Human Albumin. To determine the presence of a binding site, the specificity of the photolabeling of [^{14}C]KP to albumins was further investigated by competition experiments. The peptide-containing subdomain IIIA has a molecular mass of 11.6 kDa for human, dog, and bovine albumins, 31.8 kDa for rat albumin, and 36.0 kDa for rabbit albumin. In the absence of a competitor, the extent of radioactivity incorporation of the peptide containing subdomain IIIA for each albumin was the same as the result in Fig. 5. KP binds primarily to site II of human albumin. Site II ligands, IP, DZP, and OCT, as well as a site I ligand, WF, were used as competitors in photolabeling albumins with [^{14}C]KP. The extent of photolabeling inhibition was expressed as a percentage of the control. A decrease in the radioactivity of the peptide containing subdomain IIIA reflects the inhibition of photoincorporation of [^{14}C]KP by the competitor. In the presence of DZP and OCT, the intensity of the 11.6-kDa band of human and dog albumins decreased to an extent greater than that in the presence of IP. On the other hand, IP, DZP, and OCT reduced the radioactivity intensity of the 11.6-kDa band of bovine albumin to the same extent. WF did not appear to affect the intensity of the band containing subdomain IIIA (Fig. 6).

Determination of the Photolabeled Peptide Amino Acid Sequence of Dog Albumin. The 11.6-kDa CNBr peptide from dog albumin was subjected to further digestion with Lys-C to locate more precisely which region of subdomain IIIA was photolabeled by KP. The peptides generated from the second digestion were separated and simultaneously blotted onto a strip of PVDF membrane with a capillary HPLC system. One radioactivity spot corresponding to one peak was obtained (Fig. 7, A and B). The amino acid sequence of the photolabeled fragment after further digestion with Lys-C was XX-SESLVXRX, which corresponds to the sequence Cys^{476}-Arg^{485} of dog albumin (Fig. 7C).

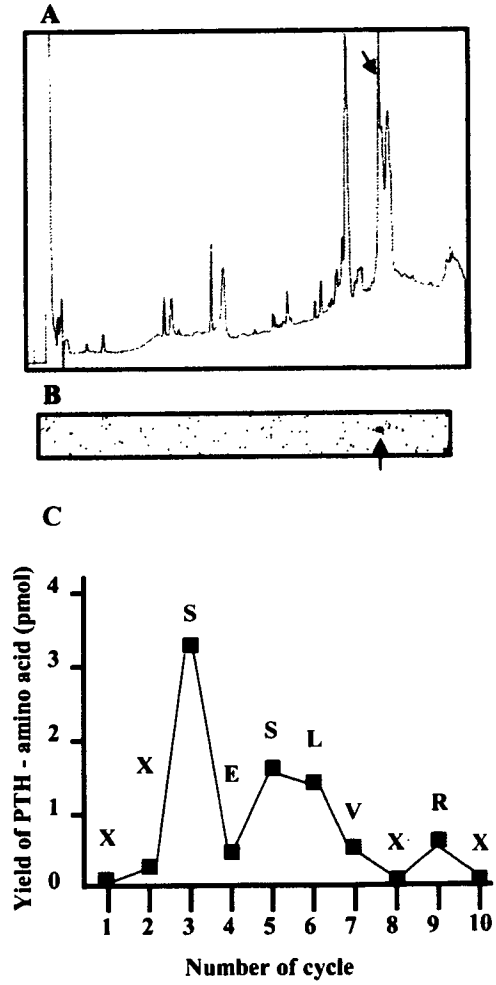

FIG. 7. Chromatogram of capillary HPLC (A), autoradiogram of blotted PVDF membrane of dog albumin digested with endopeptidase Lys-C (B), and N-terminal amino acid sequence analysis by Edman degradation method and amino acid sequence of the photolabeled region of dog albumin (C). Arrows in (A) and (B) indicate photolabeled peptide peak and radioactivity spot, respectively. PTH, phenylthiohydantoin.

Discussion

High binding affinity to a plasma protein may cause a drug to be retained in the plasma and to not be readily distributed to the tissue for therapeutic action to take place. The high degree of binding of UCN-01 to human α_1-acid glycoprotein, which causes a reduction in its distribution and clearance, resulting in high plasma concentrations in humans has been reported (Fuse et al., 1998). Moreover, we reported previously that species differences observed with phenylbutazone have an impact on the in vivo serum protein binding of sulfadimethoxine (Imamura et al., 1986).

In the process of drug development, preclinical animal trials are required to examine the safety and efficacy of the candidate drug. From the animal experiments, drug protein binding and distribution data are important for comparison of the pharmacokinetics of drugs across species and for interspecies scaling. Such comparisons will allow meaningful referencing of pharmacokinetic parameters to either

blood or plasma concentrations of the drug. Therefore, further refinement of the animal experimental design via selection of appropriate experimental animal based upon the drug class and the expected interacting proteins is desirable.

Despite the fact that the primary structure of the serum albumins of various species are highly homologous (approximately 80% homology between human and the species used in this study), drug-binding properties differ considerably among species. We reported that dog albumin is suitable for investigating drug-drug interactions on site II, whereas rat, rabbit, and bovine albumins are suitable for examining the binding of site I drugs (Kosa et al., 1997). Based on that study we attempted to elucidate the structural configuration of the binding site of dog albumin that resembles site II of HSA, using a photoaffinity labeling method (Garabedian and Yount, 1991; Chuang et al., 1999; DeSantis et al., 2000; Katsuki et al., 2005).

The usefulness of KP as a photoaffinity labeling agent and as a probe for identifying drug-binding sites on human albumin has been established previously (Chuang et al., 1999). To our knowledge, this study is the first to report identification of the presence of binding sites in various experimental animal albumins using the photoaffinity labeling technique. The extent of photoincorporation of [^{14}C]KP to each albumin was in accordance with the binding experiment result obtained with ultrafiltration and CD spectra measurements in the presence of KP (Table 1; Fig. 3). Moreover, these results are in agreement with the binding experiments using IP that we reported previously (Kosa et al., 1997) (Table 1; Figs. 1–3). The primary binding constant of KP to human albumin was similar to that reported by Rahman et al. (1993).

Autoradiographic analysis of CNBr fragments of human albumin photolabeled with [^{14}C]KP indicated that a 11.6-kDa peptide corresponding to Pro^{447}-Met^{548} contained the highest radioactivity. This sequence was found to form the binding pocket of site II in subdomain IIIA of human albumin. Dog and bovine albumins will also derive a peptide with a molecular mass of 11.6 kDa upon CNBr cleavage, as could be deduced from the amino acid sequences (Met^{446}-Met^{548}) of these two albumins. The CNBr peptides of rat and rabbit containing the sequence with high homology and that of the human albumin 11.6-kDa CNBr peptide were Met^{264}-Met^{548} (31.8 kDa) and Met^{264}-Glu^{584} (36 kDa), respectively (Fig. 4). As shown in Fig. 5, only the 11.6-kDa CNBr peptide of dog albumin incorporated radioactivity to an extent comparable to that of human albumin. Interestingly, the corresponding peptide of bovine albumin did not incorporate a significant extent of the radioactivity. Instead, a peptide with an estimated molecular mass of 15.3 kDa exhibited a higher level of radioactivity. Edman degradation of this peptide revealed an amino acid sequence starting from Pro^{447} (data not shown), indicating that the peptide might derive from an incomplete cleavage of CNBr, which resulted in a peptide with a sequence starting from Pro^{447}-Ala^{584}. It is very likely that Met^{548} of bovine albumin could have been photolabeled by [^{14}C]KP, resulting in its resistance to CNBr cleavage.

Such a discrepancy could be due to a difference in the amino acid sequence that would notably influence the secondary as well as the tertiary structures of the albumins. The induced CD spectra for KP binding (Fig. 2) and the intrinsic CD spectra for albumins themselves showed a difference between human albumin and bovine albumin (data not shown), in agreement with the results reported by Kosa et al. (1997). Hence, human, dog, and bovine albumins contain a binding site of KP in subdomain IIIA, but the binding site structural configuration of bovine albumin is somewhat different from those of human and dog albumins.

IP, DZP, and OCT, site II ligands of human albumin, were able to inhibit the binding of KP to the primary binding sites of dog and bovine albumins. However, the inhibition pattern suggested that KP interacted with dog albumin in a manner similar to that for human albumin but different from that for bovine albumin (Fig. 6). In a previous study, we reported that bovine albumin has no primary but only a secondary binding site for DZP (Kosa et al., 1997). Hence, this secondary binding site of DZP might overlap with the binding site of KP on bovine albumin. The inhibition pattern of human albumin and hence that of dog albumin by IP, DZP, and OCT could be explained from the crystal structures of the drug-HSA complex (Ghuman et al., 2005). We previously reported that the hydrophobic moiety of *R*-KP interacts with Arg^{485} (Chuang et al., 1999). In the IP-human albumin complex crystal structures, IP binds in the site II binding pocket in such a way that its hydrophobic moiety was away from Arg^{485} in contrast to DZP, which binds near to Arg^{485} (Ghuman et al., 2005). Bhattacharya et al. (2000) proposed that two molecules of medium chain fatty acids, including OCT, bind to site II and one of the two molecules forms hydrogen bond to Arg^{485}. This proposal may provide an explanation for the observation that IP inhibited KP binding to a lesser extent than did DZP and OCT.

TABLE 2

The amino acid sequence of peptide (476–499) of albumin of different species

Species	Peptide of 476–499	Homology	Primary Binding Sites	
		%		
Human	CCTESLVNRRPCFSALEVDETYVPK		IP*	DZP*
Dog	CCSESLVNRRPCFSGLEVDETYVPK	91.7	O	O
Bovine	CCTESLVNRRPCFSALTPDETYVPK	91.7	O	X
Rat	CCSGSLVERRPCFSALTVDETYVPK	83.3	O	X
Rabbit	CCSESLSNRRPCFSALGPDETYVPK	83.3	O	X

* Kosa et al., 1997.

Amino acid sequence analysis of the photolabeled peptide of dog albumin after further digestion with Lys-C enzyme indicated a sequence corresponding to the sequence Cys^{476}-Pro^{499} of dog albumin (Fig. 7C). In a previous study, we reported that Cys^{476}-Pro^{499} in subdomain IIIA (site II) of human albumin was the region photolabeled by KP (Chuang et al., 1999). Sequence homology comparison of this Cys^{476}-Pro^{499} peptide of human albumin (Chuang et al., 1999) and dog albumin (Fig. 7C), with all other albumins used in the study showed that dog and bovine albumin has the highest homology (91.7%) with human albumin. As shown in Table 2, human and dog albumins have Glu^{492} and Val^{493}, but bovine albumin does not. Moreover, DZP, a site II ligand, binds to dog albumin with high affinity but only binds to bovine albumin with much lower affinity (Kosa et al., 1997). Thus, Glu^{492} and Val^{493} in human and dog albumins are important residues that constitute the structure of the site II binding site. In addition, the induced CD spectra of the human albumin-KP complex agreed with that of the dog albumin-KP complex (Fig. 2). The CD spectra of these albumins indicated that the secondary and tertiary structures of dog albumin were almost the same as those of human albumin (data not shown). Therefore, dog albumin contains a binding site located in subdomain IIIA exhibiting a structural configuration of binding similar to that of site II of human albumin.

In conclusion, in the preclinical animal experiments, dog may be a better candidate animal for examination of the protein binding as well as distribution of site II drugs.

Acknowledgments. We thank members of Kumamoto University Institute of Resource Development and Analysis Radioisotope Center.

References

Acharya MR, Sparreboom A, Sausville EA, Conley BA, Doroshow JH, Venitz J, and Figg WD (2006) Interspecies differences in plasma protein binding of MS-275, a novel histone deacetylase inhibitor. *Cancer Chemother Pharmacol* **57**:275–281.

Bhattacharya AA, Grune T, and Curry S (2000) Crystallographic analysis reveals common modes of binding of medium and long-chain fatty acids to human serum albumin. *J Mol Biol* **303**:721–732.

Chuang VT, Kuniyasu A, Nakayama H, Matsushita Y, Hirono S, and Otagiri M (1999) Helix 6 of subdomain III A of human serum albumin is the region primarily photolabeled by ketoprofen, an arylpropionic acid NSAID containing a benzophenone moiety. *Biochim Biophys Acta* **1434**:18–30.

Curry S, Mandelkow H, Brick P, and Franks N (1998) Crystal structure of human serum albumin complexed with fatty acid reveals an asymmetric distribution of binding sites. *Nat Struct Biol* **5**:827–835.

Davi H, Tronquet C, Caix J, Simiand J, Briot C, Berger Y, and Thiercelin JF (1999) Disposition of tiludronate (Skelid) in animals. *Xenobiotica* **29**:1017–1031.

DeSantis G, Paech C, and Jones JB (2000) Benzophenone boronic acid photoaffinity labeling of subtilisin CMMs to probe altered specificity. *Bioorg Med Chem* **8**:563–570.

Dubois N, Lapicque F, Magdalou J, Abiteboul M, and Netter P (1994) Stereoselective binding of the glucuronide of ketoprofen enantiomers to human serum albumin. *Biochem Pharmacol* **48**:1693–1699.

Fuse E, Tanii H, Kurata N, Kobayashi H, Shimada Y, Tamura T, Sasaki Y, Tanigawara Y, Lush RD, Headlee D, et al. (1998) Unpredicted clinical pharmacology of UCN-01 caused by specific binding to human α_1-acid glycoprotein. *Cancer Res* **58**:3248–3253.

Garabedian TE and Yount RG (1991) Direct photoaffinity labeling of gizzard myosin with vanadate-trapped adenosine diphosphate. *Biochemistry* **30**:10126–10132.

Ghuman J, Zunszain PA, Petitpas I, Bhattacharya AA, Otagiri M, and Curry S (2005) Structural basis of the drug-binding specificity of human serum albumin. *J Mol Biol* **353**:38–52.

Ho JX, Holowachuk EW, Norton EJ, Twigg PD, and Carter DC (1993) X-ray and primary structure of horse serum albumin (*Equus caballus*) at 0.27-nm resolution. *Eur J Biochem* **215**:205–212.

Imamura Y, Nakamura H, and Otagiri M (1986) Effect of phenylbutazone on serum protein binding of sulfadimethoxine in different animal species. *J Pharmacobiodyn* **9**:694–696.

Katsuki M, Chuang VT, Nishi K, Kawahara K, Nakayama H, Yamaotsu N, Hirono S, and Otagiri M (2005) Use of photoaffinity labeling and site-directed mutagenesis for identification of the key residue responsible for extraordinarily high affinity binding of UCN-01 in human α_1-acid glycoprotein. *J Biol Chem* **280**:1384–1391.

Kosa T, Maruyama T, and Otagiri M (1997) Species differences of serum albumins: I. Drug binding sites. *Pharmacol Res* **14**:1607–1612.

Lewis RE, Wiederhold NP, Prince RA, and Kontoyiannis DP (2006) In vitro pharmacodynamics of rapid versus continuous infusion of amphotericin B deoxycholate against *Candida* species in the presence of human serum albumin. *J Antimicrob Chemother* **57**:288–293.

Mizojiri K, Okabe H, Sugeno K, Misaki A, Ito M, Kominami G, Esumi Y, Takaichi M, Harada T, Seki H, et al. (1997) Studies on the metabolism and disposition of the new retinoid 4-[(5,6,7,8-tetrahydro-5,5,8,8-tetramethyl-2-naphthyl)carbamoyl] benzoic acid. 4th communication: absorption, metabolism, excretion and plasma protein binding in various animals and man. *Arzneimittelforschung* **47**:259–269.

Nonaka K, Tsujioka T, Tougou K, and Mukai H (2003) Pharmacokinetics of the new pyrimidine derivative NS-7, a novel Na^+/Ca^{2+} channel blocker. 1st communication: plasma concentrations and excretions after a single intravenous ^{14}C-NS-7 injection to rats, dogs and monkeys. *Arzneimittelforschung* **53**:612–620.

Peters, T (1996) *All About Albumin*. Academic Press, San Diego.

Petersen CE, Ha CE, Curry S, and Bhagavan NV (2002) Probing the structure of the warfarin-binding site on human serum albumin using site-directed mutagenesis. *Proteins* **47**:116–125.

Petitpas I, Petersen CE, Ha CE, Bhattacharya AA, Zunszain PA, Ghuman J, Bhagavan NV, and Curry S (2003) Structural basis of albumin-thyroxine interactions and familial dysalbuminemic hyperthyroxinemia. *Proc Natl Acad Sci U S A* **100**:6440–6445.

Rahman MH, Yamasaki K, Shin YH, Lin CC, and Otagiri M (1993) Characterization of high affinity binding sites of non-steroidal anti-inflammatory drugs with respect to site-specific probes on human serum albumin. *Biol Pharm Bull* **16**:1169–1174.

Simard JR, Zunszain PA, Hamilton JA, and Curry S (2006) Location of high and low affinity fatty acid binding sites on human serum albumin revealed by NMR drug-competition analysis. *J Mol Biol* **361**:336–351.

Sudlow G, Birkett DJ, and Wade DN (1975) The characterization of two specific drug binding sites on human serum albumin. *Mol Pharmacol* **11**:824–832.

Weiss HM, Fresneau M, Camenisch GP, Kretz O, and Gross G (2006) In vitro blood distribution and plasma protein binding of the iron chelator deferasirox (ICL670) and its iron complex Fe-[ICL670]2 for rat, marmoset, rabbit, mouse, dog, and human. *Drug Metab Dispos* **34**:971–975.

Zandomeneghi M (1995) Circular dichroism of ketoprofen complexed to serum albumins: conformational selection by the protein: a novel optical purity determination technique. *Chirality* **7**:446–451.

Address correspondence to: Dr. Masaki Otagiri, Department of Biopharmaceutics, Graduate School of Pharmaceutical Sciences, Kumamoto University, 5-1 Oe-honmachi, Kumamoto 862-0973, Japan. E-mail: otagirim@gpo.kumamoto-u.ac.jp

Available online at www.sciencedirect.com
ScienceDirect
Biochemical and Biophysical Research Communications 364 (2007) 790–795
BBRC
www.elsevier.com/locate/ybbrc

Effects of endogenous ligands on the biological role of human serum albumin in S-nitrosylation ☆

Yu Ishima [a], Takaaki Akaike [b], Ulrich Kragh-Hansen [c], Shuichi Hiroyama [a], Tomohiro Sawa [b], Toru Maruyama [a], Toshiya Kai [a], Masaki Otagiri [a,*]

[a] *Department of Biopharmaceutics, Graduate School of Pharmaceutical Sciences, Kumamoto University, 5-1 Oe-honmachi, Kumamoto 862-0973, Japan*
[b] *Department of Microbiology, Graduate School of Medical Sciences, Kumamoto University, 1-1-1 Honjo, Kumamoto 860-0811, Japan*
[c] *Department of Medical Biochemistry, University of Aarhus, DK-8000 Aarhus C, Denmark*

Received 9 October 2007
Available online 26 October 2007

Abstract

Many proteins have been identified as targets for S-nitrosylation, including structural and signaling proteins, and ion channels. S-nitrosylation plays an important role in regulating their activity and function. We used human serum albumin (HSA), a major endogenous NO traffic protein, and studied the effect of mediators on S-nitrosylation processes which control NO bioactivity. By using NOC-7, S-nitrosoglutathione, and activated RAW264.7 cells as NO-donors we found that high-affinity binding of endogenous ligands (Cu^{2+}, bilirubin and fatty acid) can affect these processes. It is likely that the same effects take place in many clinical situations characterized by increased fatty acid concentrations in plasma such as type II diabetes and the metabolic syndrome. Thus, endogenous ligands, changing their plasma concentrations, could be a novel type of mediator of S-nitrosylation not only in the case of HSA but also for other target proteins.

Keywords: Human serum albumin; Nitric oxide; Type II diabetes; Metabolic syndrome; Cysteine; S-Nitrosylation; Ligand binding; Fatty acids; Copper; Bilirubin

Post-translational modifications are essential in their functional regulation. Among these, changes of the redox state of cysteine residues are of great importance. The sulfhydryl moiety can interact with nitric oxide (NO) and thereby form S-nitrosothiols (RS-NO) [1–3]. RS-NOs may function as NO reservoirs and preserve the antioxidant and other activities of NO [4,5]. For example, it has been reported that S-nitroso human serum albumin (SNO-HSA) may serve in vivo as a circulating reservoir for NO produced by the endothelial cells [6]. The reservoir function was also reported to be operative when application of SNO-HSA to animals suffering from ischemia-reperfusion injury minimized the extent of tissue damage associated with reperfusion [7,8]. However, several pieces of evidence propose that RS-NOs are more than simply NO reservoirs [4]. Thus, the antibacterial and cytoprotective properties of SNO-HSAs [9] are most probably the results of S-transnitrosylation.

HSA is a single, non-glycosylated polypeptide that organizes to form a heart-shaped protein with approximately 67% α-helix but no β-sheet [10]. All but one (Cys-34) of the 35 cysteine residues are involved in the formation of

Abbreviations: HSA, human serum albumin; SNO-HSA, S-nitroso HSA; RS-NOs, S-nitrosothiols; GSH, glutathione; GS-NO, S-nitrosoglutathione; NOC-7, 1-hydroxy-2-oxo-3-(*N*-3-methyl-aminopropyl)-3-methyl-3′-triazene; OA, oleic acid; BR, bilirubin; DTT, 1,4-dithiothreitol; DTNB, 5,5′-dithiobis-2-nitrobenzoic acid; DTPA, diethylenetriaminepentaacetic acid; EDTA, ethylenediaminetetraacetic acid; PBS, phosphate-buffered saline; NEM, *N*-ethylmaleimide.

☆ This work was supported in part by Grants-in-Aid from the Japan Society for the Promotion of Science (JSPS), a Grant-in-Aid from the Ministry of Education, Culture, Sports, Science and Technology (18390051), Japan, and by Fonden af 1870.

* Corresponding author. Fax: +81 96 362 7690.
E-mail address: otagirim@gpo.kumamoto-u.ac.jp (M. Otagiri).

0006-291X/$ - see front matter © 2007 Elsevier Inc. All rights reserved.
doi:10.1016/j.bbrc.2007.10.094

stabilizing disulfide bonds. In the circulation, normally about half of the Cys-34 residues are freely accessible, i.e., not oxidized or involved in ligand binding, and they represent the largest fraction of free thiols in blood.

HSA is the most abundant protein in blood plasma and serves, among other things, as a transport and depot protein for numerous endogenous and exogenous compounds [10]. We studied the effects of the strongly bound ligands oleate (OA), bilirubin (BR) and Cu^{2+} and the weakly bound ligands L-tryptophan, progesterone, ascorbate, Zn^{2+} and Fe^{2+} on S-nitrosylation of HSA by S-nitrosoglutathione (GS-NO), 1-hydroxy-2-oxo-3-(N-3-methyl-aminopropyl)-3-methyl-3′-triazene (NOC-7) and stimulated RAW264.7 cells.

Materials and methods

Materials. Non-defatted HSA (96% pure) was donated by the Chemo-Sera-Therapeutic Research Institute (Kumamoto, Japan), and it was defatted by treatment with charcoal as described by Chen [11]. Sephadex G-25 (φ1.6 × 2.5 cm), Blue Sepharose CL-6B (φ2.5 × 20 cm), and RESOURCE PHE columns (φ0.64 × 3 cm) were from Amersham Pharmacia Biotech (Tokyo, Japan). Enzymes for DNA assays were from Takara (Kyoto, Japan). The Pichia Expression kit was from Invitrogen (Carlsbad, CA). L-Tryptophan, ascorbic acid, $FeCl_2$, $(CH_3COO)_2Zn$, $CuSO_4{\cdot}5H_2O$, BR, progesterone, OA, 1,4-dithiothreitol (DTT), and glutathione (GSH) were purchased from Sigma–Aldrich (St. Louis, MO). Sulfanilamide, naphthylethylenediamine–hydrochloride, $HgCl_2$ and $NaNO_2$ were obtained from Nakalai Tesque (Kyoto, Japan). GS-NO, NOC-7, 5,5′-dithiobis-2-nitrobenzoic acid (DTNB), diethylenetriaminepentaacetic acid (DTPA), and ethylenediaminetetraacetic acid (EDTA) were obtained from Dojindo Laboratories (Kumamoto, Japan). Other chemicals were of the best grades commercially available, and all solutions were made in deionized and distilled water.

Synthesis and purification of recombinant HSA. Wild-type HSA and the H3A mutant were synthesized, using *P. pastoris* GS115 his4, and purified as previously described [9]. The mutagenic primers (sense and antisense) for making the mutant were:

5′-GCTCATCCGATGGCCACAAGAGTGAGG-3′, and 3′-CCTCA CTCTTGTGGCCATCGGATGAGC-5′.

The albumins were deionized and defatted via charcoal treatment, freeze-dried, and then stored at −20 °C until used. According to density analysis of Coomassie Brilliant Blue-stained protein bands on 12.5% SDS–PAGE, the purity of the protein samples were more than 97%.

Preparation of ligand-HSA solutions. First, HSA was treated with DTT as follows. HSA (300 μM) was incubated with DTT (molar ratio, protein:DTT = 1:10) for 5 min at 37 °C. After that, DTT was quickly removed by Sephadex G-25 gel filtration using 10 mM phosphate-buffered saline (pH 7.4) (PBS; Ca^{2+}, Mg^{2+} free). Stock solutions of 20 mM OA and 20 mM progesterone were made in methanol-H_2O (1:1, v/v) and ethanol-H_2O (1:1, v/v), respectively, whereas 20 mM BR was made in 0.1 N NaOH and protected against light. Later, these stock-solutions were diluted with PBS. Other ligands were directly dissolved in PBS. In all cases, the resulting solutions were mixed with PBS containing HSA. The ligand–protein solutions, except for those having $CuSO_4$, were incubated for 30 min at 37 °C in the dark. Freshly prepared $CuSO_4$-HSA solutions were also incubated for 30 min in the dark but at 4 °C, because the SH-group of HSA easily undergoes oxidation in the presence of Cu^{2+}. To remove free ligands, mixtures were applied to a Sephadex G-25 column, quickly eluted with PBS and concentrated by ultrafiltration. The protein content of all protein preparations used in this study was determined by the Bradford assay.

Accessibility of Cys-34. In reduced HSA this was estimated with Ellman's reagent, DTNB. Briefly, the accessibility was evaluated as A_5/A_{60}, where A_5 and A_{60} is the sample absorbance at 405 nm after 5 min and 60 min (maximal absorbancy), respectively, of incubation with DTNB [12].

S-Nitrosylation of HSA in cell-free reaction systems. SNO-HSA was prepared with protection against light and according to previous reports [13,14]. HSA (100 μM) with and without ligand was incubated with GS-NO or NOC-7 as NO donor (molar ratio, protein:NO donor = 1:5) in PBS for 10 min at 37 °C. To remove NO donors, S-nitrosylated products were applied to a Sephadex G-25 column, eluted with PBS containing 0.5 mM DTPA, and concentrated by ultrafiltration. These samples were stored at −80 °C until analyzed.

Determination of S-nitrosylation efficiency. The amounts of the S-nitroso moiety of SNO-HSA were quantified by HPLC coupled with a flow-reactor system, as previously reported [13,15]. The HPLC column was a gel filtration column for S-nitrosylated proteins (φ8 × 300 mm), Diol-120, YMC, Kyoto, Japan. Briefly, the eluate from the HPLC column was mixed with a $HgCl_2$ solution to decompose S-nitrosylated compounds to yield NO_2^- (via NO^+). The NO_2^- generated was then detected after reaction with Griess reagent in the flow-reactor system.

SNO-HSA production by cells in culture. RAW264.7 cells were cultured in 24-well plates (16-mm diameter; Falcon, Lincoln Park, NJ) with Dulbecco's modified Eagle's medium supplemented with 10% fetal bovine serum and nonessential amino acids (Life Technologies, Inc.). Cells at saturation density (1×10^6 cells/well) were stimulated with interferon-γ (Genzyme, Cambridge, MA) at 100 U/ml and lipopolysaccharide (*Escherichia coli* 026B; Difco) at 10 μg/ml for 12 h at 37 °C in a CO_2 incubator (5% CO_2, 95% air (v/v)). The culture medium was removed, and the cells were washed three times with PBS (pH 7.4). Cells were further incubated in the CO_2 incubator at 37 °C with 200 μl of PBS containing 0.5 mM L-arginine and 100 μM HSA alone or with bound ligand. After incubation for 10 min, the reaction medium was mixed with 1/10 volume of 5 mM DTPA dissolved in PBS (pH 7.4), followed by centrifugation at 10,000*g* for 10 min at 4 °C. The resultant supernatants were stored at −80 °C until applied to the HPLC-flow reactor system.

Statistical analysis. The statistical significance of collected data was evaluated using the ANOVA analysis followed by Newman–Keuls method for more than 2 means. Differences between groups were evaluated by the Student's *t* test. $P < 0.05$ was regarded as statistically significant.

Results and discussion

S-Nitrosylation of mercaptalbumin with bound ligands

HSA purified from serum has bound endogenous ligands, in particular fatty acids, and perhaps also exogenous ligands. Any effect of these ligands on the S-nitrosylation of HSA was examined by incubating non-defatted and charcoal-treated albumin with GS-NO. The S-nitroso moiety of the former preparation was 0.41 ± 0.02 ($n = 4$), whereas that of the latter was only 0.19 ± 0.01 ($P < 0.01$). Thus, the presence of ligands greatly enhanced the efficiency of S-nitrosylation. In order to identify ligands of importance for S-nitrosylation, individual ligands were added to HSA, which had been delipidated by charcoal and dialyzed extensively against deionized water. In these experiments, two kinds of S-nitrosylating agents were used, namely GS-NO which S-transnitrosylates via NO^+, and NOC-7 which S-nitrosylates mainly via NO and N_2O_3. The results obtained with equimolar amounts of protein and ligand are given in Figs. 1A and 2A. It can be seen that OA and BR enhances the efficiency of GS-NO, but not that of NOC-7, whereas Cu^{2+} increases the S-nitrosylation by NOC-7 but not that caused by GS-NO. In contrast, no significant effect was observed when adding L-tryptophan,

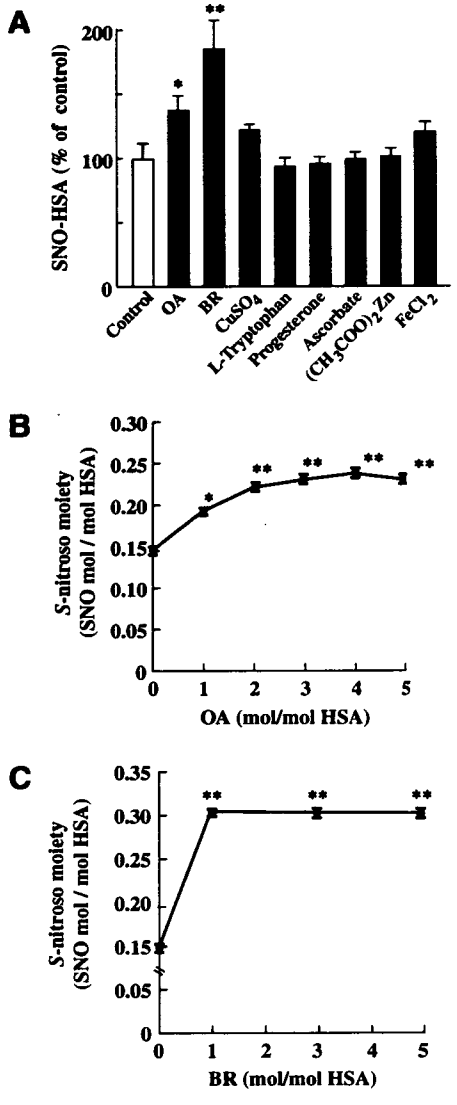

Fig. 1. Effect of ligand binding on S-nitrosylation of HSA by GS-NO. (A) 100 μM DTT-treated HSA was incubated with 100 μM of different ligands. (B) DTT-treated HSA was incubated with different molar ratios of OA. (C) DTT-treated HSA was incubated with different molar ratios of BR. In all cases, the GS-NO concentration was 500 μM. Data are expressed as means ± SEM ($n = 4$–6). $^{*}P < 0.05$, $^{**}P < 0.01$, as compared with control.

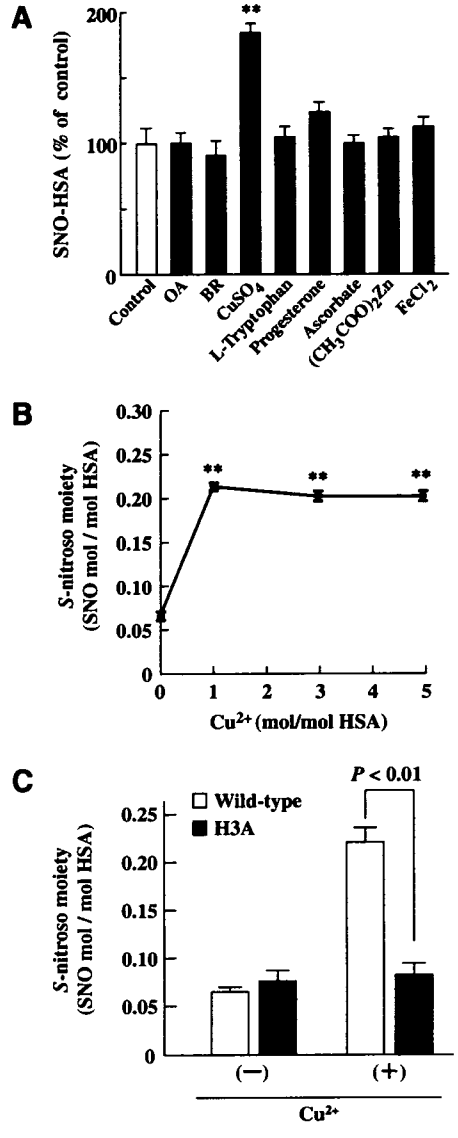

Fig. 2. Effect of ligand binding on S-nitrosylation of HSA by NOC-7. (A) Hundred micromolars of DTT-treated HSA was incubated with 100 μM of different ligands. (B) DTT-treated HSA was incubated with different molar ratios of Cu^{2+}. (C) Wild-type HSA and the H3A mutant, without or with Cu^{2+}, were S-nitrosylated by NOC-7. In all cases, the NOC-7 concentration was 500 μM. Data are expressed as means ± SEM ($n = 4$–6). $^{**}P < 0.01$, as compared with control.

progesterone, ascorbate, $(CH_3COO)_2Zn$ or $FeCl_2$. In the following, we have studied in more detail the positive effects of OA, BR and Cu^{2+}, which bind to different high-affinity sites of HSA [10,16] (Fig. 3).

Fig. 1B shows an increasing effect of OA on S-nitrosylation of HSA by GS-NO. The increment is dose-dependent until a OA:HSA molar ratio of 3; increasing the molar ratio further to 4 or 5 did not result in additional S-nitrosylation. Because OA does not bind to Cys-34 (Fig. 3), the effect observed could be due to binding-induced conformational changes of HSA making Cys-34 more accessible to GS-NO [12,17]. Actually, the data given in Table 1 propose such a mechanism, because OA binding results in an almost linear increment in binding of the test-compound DTNB to Cys-34.

The effect of BR binding on S-nitrosylation by GS-NO was also studied at different molar ratios of ligand to protein (Fig. 1C). Without BR the amount of S-nitroso moieties was 0.15 ± 0.02 ($n = 3$), and with BR it was approximately 0.30 ($P < 0.01$). The latter value was obtained, whether the BR:HSA molar ratio was 1, 3 or 5. Thus, only high-affinity BR binding increases S-nitrosylation. Because this kind of binding takes place to another region of HSA than that housing Cys-34 (Fig. 3) the improving effect must be the result of conformational

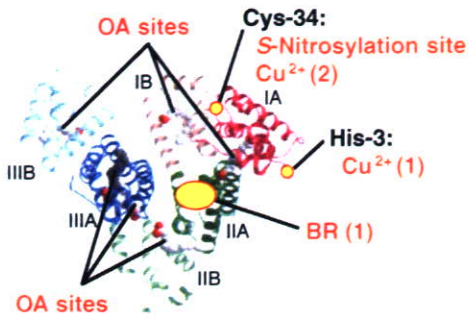

Fig. 3. Crystal structure of HSA showing locations of OA binding sites, high-affinity binding sites for BR (BR(1)) and Cu^{2+} ($Cu^{2+}(1)$) and Cys-34 which also is the site for secondary Cu^{2+} binding ($Cu^{2+}(2)$). The subdivision of HSA into domains (I-III) and subdomains (A and B) is indicated. The structure was simulated on the basis of X-ray crystallographic data for HSA-OA (PDB ID code 1gni) and modified with the use of Rasmol (downloaded from http://www.openrasmol.org).

Table 1
Effect of binding on the accessibility of Cys-34

Ligand/HSA	0	1	3	5
OA	0.17 ± 0.01	$0.22 \pm 0.02^{*}$	$0.67 \pm 0.03^{**}$	$0.84 \pm 0.04^{**}$
BR	0.17 ± 0.02	N.D.	N.D.	N.D.
Cu^{2+}	0.17 ± 0.02	0.18 ± 0.03	0.20 ± 0.04	0.19 ± 0.04

The accessibility was evaluated as A5/A60, where A5 and A60 is the sample absorbance at 405 nm after 5 min and 60 min (maximal absorbancy), respectively, of incubation with DTNB [12]. Results are given as means ± SEM ($n = 5$). N.D., not determined. $^{*}P < 0.05$, $^{**}P < 0.01$, as compared with Ligand/HSA = 0.

changes in the protein related to accommodation of the large BR molecule. That such conformational changes take place has previously been detected by techniques such as fluorescence spectroscopy [10]. By contrast to GS-NO, high-affinity binding of BR does not influence S-nitrosylation by NOC-7 (Fig. 2A). For testing whether this lack of effect could be caused by an interaction between NO and HSA-bound BR, we performed spectrophotometric experiments. These experiments showed that exposure of HSA-BR to NOC-7, but not to GS-NO, results in a fast decrease of the absorbancy at 470 nm (representing λ_{max} for HSA-BR) and a concomitant and pronounced increase at 650 nm (representing λ_{max} for HSA-biliverdin) (data not shown). Therefore, the following reaction seems to have taken place: (^{34}Cys-SH)-HSA-BR + ·NO → (^{34}Cys-SH)-HSA-BV + NO_2^-. Thus, the lack of effect of BR is due to a conversion to biliverdin (BV), and neither that ligand nor the NO_2^- formed can improve S-nitrosylation.

In contrast to the S-nitrosylating effect of GS-NO, the effect of NOC-7 was significantly increased by the presence of Cu^{2+} (Fig. 2A). The increasing effect was the same, whether the molar ratio of Cu^{2+} to protein was 1:1, 3:1 or 5:1 (Fig. 2B). Cu^{2+} binds with a very high affinity to a specific site in the N-terminal region of HSA, and His-3 is an essential element of that site [10]. In order to test whether high-affinity binding of Cu^{2+}, which takes place at a distance from Cys-34 (Fig. 3), is responsible for the improving effect of NOC-7, or whether the effect is caused by other means, e.g. secondary binding, we mutated His-3 for an alanine. The results of Fig. 2C show that the positive effect of Cu^{2+} disappears when mutating His-3. This finding strongly proposes high-affinity binding as the reason for the improving effect of Cu^{2+} on the S-nitrosylation by NOC-7. The positive effect of high-affinity Cu^{2+} binding is most probably caused by conformational changes induced in the HSA molecule, which render the SH-group of Cys-34 more reactive. Such a mechanism also seems to be supported by the results of Zhang and Wilcox [18]. These authors, using isothermal titration calorimetry and different spectroscopic techniques, found evidence for an interaction between the first Cu^{2+} binding site and Cys-34 in bovine serum albumin. However, these conformational changes are different from those caused by OA, because in contrast to OA binding of Cu^{2+} does not affect the accessibility of Cys-34 (Table 1). In contrast to the present findings Stubauer et al. [19] found no effect of high-affinity bound Cu^{2+} on RS-NO formation. RS-NO formation was only initiated, when that binding site was saturated, and the authors proposed S-nitrosylation of Cys-34 when also Cu^{2+} binds with a low affinity to the same residue. However, they used bovine serum albumin and NO gas in their studies.

S-Nitrosylation of mercaptalbumin-ligand complexes by NOC-7 and RAW264.7 cells

For studying S-nitrosylation of HSA in a biological system, we investigated the process caused by the murine macrophage cell line RAW264.7 (Fig. 4). The cell line had been activated by interferon-γ and lipopolysaccharide for expressing the inducible NO synthase. Binding of OA or BR does not affect S-nitrosylation of HSA by the cells. By contrast, Cu^{2+} binding facilitates S-nitrosylation (Fig. 4B). Fig. 4C shows that binding of Cu^{2+}, but not binding of OA or BR, decreases significantly the production of NO_2^-. These results propose that the formation of SNO-HSA by the cell line takes place via NO. This proposal was supported by findings showing that the effects of GS-NO in a similar experiment were different from those of NOC-7 and the RAW cells (data not shown).

Concluding remarks

Normally, the molar ratio of endogenous fatty acids to HSA is about 1.5 or lower [10], and those of BR and Cu^{2+} are below unity. Strenuous exercise or other adrenergic stimulation can rise the molar ratio for fatty acids to about 4 [10]. The molar ratios of all three ligands can be elevated in pathological conditions, e.g., metabolic syndrome, Type II (non-insulin-dependent) diabetes (fatty acids), increased catabolism of hemoglobin or hepatic